University of Texas at El Paso
DigitalCommons@UTEP

Open Access Theses & Dissertations

2015-01-01

Evaluation Of Small Molecules On The Excitatory Amino Acid Transporter 3 (eaat3) For The Treatment Of OCD

Emmanuel Zubia
University of Texas at El Paso, ezubia@miners.utep.edu

Follow this and additional works at: https://digitalcommons.utep.edu/open_etd

 Part of the Biochemistry Commons, and the Chemistry Commons

Recommended Citation
Zubia, Emmanuel, "Evaluation Of Small Molecules On The Excitatory Amino Acid Transporter 3 (eaat3) For The Treatment Of OCD" (2015). *Open Access Theses & Dissertations*. 1184.
https://digitalcommons.utep.edu/open_etd/1184

This is brought to you for free and open access by DigitalCommons@UTEP. It has been accepted for inclusion in Open Access Theses & Dissertations by an authorized administrator of DigitalCommons@UTEP. For more information, please contact lweber@utep.edu.

EVALUATION OF SMALL MOLECULES ON THE EXCITATORY AMINO ACID TRANSPORTER 3 (EAAT3) FOR THE TREATMENT OF OCD

EMMANUEL ZUBIA SALGADO
Department of Chemistry

APPROVED:

_____
Mahesh Narayan, Ph.D., Chair

_____
Juan C. Noveron, Ph.D.

_____
Binata Joddar, Ph.D.

_____
Charles H. Ambler, Ph.D.
Dean of the Graduate School

Copyright ©

by

Emmanuel Zubia

2015

DEDICATION

Friends and Family

EVALUATION OF SMALL MOLECULES ON THE EXCITATORY AMINO ACID TRANSPORTER 3 (EAAT3) FOR THE TREATMENT OF OCD

by

EMMANUEL ZUBIA SALGADO, B.S.

THESIS

Presented to the Faculty of the Graduate School of

The University of Texas at El Paso

in Partial Fulfillment

of the Requirements

for the Degree of

MASTER OF SCIENCE

Department of Chemistry

THE UNIVERSITY OF TEXAS AT EL PASO

December 2015

ACKNOWLEDGEMENTS

There are many people in my life without whom I would have failed terribly in pursuing my academic career and personal development. I dedicate this work to my loving wife Bere, who has helped me tremendously in my research and the writing of thesis; to my parents Elisa Salgado and Eduardo Zubia, without whom I would not be the gentleman I am today; and to my siblings, without whose encouragement and advice I would not have been able to complete this degree. A special thanks to Dr. Mahesh Narayan, my graduate advisor and mentor who has guided me through my career and has helped me persevere in this academic path. Finally, I would like to thank my friends Ricardo McCreary and Dr. Gustavo Avila, who made my academic career easier to go through.

ABSTRACT

We seek to discover new drug candidates for the excitatory amino acid transporter 3 (EAAT3) for the treatment of Obsessive Compulsive Disorder (OCD). We hypothesize that decreasing the glutamatergic transmission via EAAT3 intervention will create an amelioration of the symptoms of OCD. For this we have prepared in-silico binding calculations to identify a better compound that can stimulate EAAT3 and decrease glutamatergic transmission. This research will help us further understand and elucidate the role of glutamate in the neural mechanisms of this illness, which to date remain inconclusive. Those areas of study are significant because, until now, there is no effective medication for patients with OCD. Currently, the first line of medication is the use of serotonin reuptake inhibitors (SRI); however, most of the patients undergoing treatment still experience some of the symptoms.

TABLE OF CONTENTS

LIST OF TABLES

LIST OF FIGURES

CHAPTER 1: INTRODUCTION

1.1. Introduction to Obsessive Compulsive Disorder

Obsessive Compulsive Disorder (OCD) is a neurological disease that is characterized by persistent, unwanted thoughts (obsessions) and routines or ritualistic behaviors (compulsions).[1,2] Generally this disease does not originate from a traumatic experience, but rather the onset of the disorder seems to be pervasive and gradual. The symptoms often change over time, but there is no direct link between an initial traumatic event and a symptom.[2,3] Individuals affected by OCD suffer from intrusive thoughts that lead to an increase in anxiety, from which they find it very difficult to avoid adopting certain behaviors. Even though the affected individuals might find the behavior inappropriate and stressful, they cannot control it.[4,3] Symptoms of OCD may be motivated by factors other than fear, such as feelings of incompleteness or "not just right" experiences.[5] If left untreated, OCD can become a disabling and chronic illness.[3,6] Through empirical research,[5] this illness can be divided into four different subtypes as shown in table 1. One example of OCD of the contamination subtype is the case of a man with OCD that was washing and polishing his neighbors' automobiles without permission. He was arrested but was later released when he explained to the officers that he had OCD. On his way out of the station, he began cleaning the police cars.[4]

Table 1. Summary of the different types of behaviors shown in OCD.

Contamination	• Characterized with the feeling of contamination with the obsession of excessive cleaning or washing. • This is the most common subtype of OCD.
Symmetry	• Characterized by concerning with symmetry/precision and have the compulsion of ordering, arranging, and counting. • The second most common subtype of OCD.
***Hoarding**	• Characterized by difficulty in discarding items, (often appear worthless to others) and have the compulsion of collecting items. • Third most common and often the most disabling of all forms of OCD.
Harming	• Characterized by presence of intrusive thoughts often sexual, religious, aggressive or somatic nature however without overt compulsion, these intrusive thoughts are appraised as important by their mere occurrence. • Prevalence rate suggest that it is not a common subtype of OCD.

** Until recently, The American Psychiatric Association Diagnostic and Statistical Manual for Mental Disorders fifth edition (DMS-5), has categorized Hoarding as a distinct anxiety disorder under the category of OCD-related.*

It is known that OCD is comorbid with various mental illnesses; amongst them, the disorder with the highest comorbidity with OCD is Tourette's Syndrome (TS). Individuals with TS have a 50% chance of developing OCD.[7,2,5] Other disorders that are also comorbid with OCD include: Autism Spectrum Disorders (ASDs), Unipolar Mood Disorder, Schizophrenia, Huntington's Disease, Sydenham's Chorea, Attention-Deficit/Hyperactivity Disorder (ADHD), Depression, Addiction, Post-Traumatic Stress Disorder (PTSD), Generalized Anxiety Disorder, Panic Disorder, and Social Phobia.[4,2,8,9,10,11] The direct correlation between OCD and other mental illnesses is not well understood; however, these previously mentioned disorders might share a common dysfunction in similar areas of the brain.

In OCD, compulsions may serve to prevent increasing anxiety levels after encountering a trigger; paradoxically, the compulsions can make the individual uncomfortable and, as a result, elevate anxiety. Figure 1 gives an illustration of the OCD process. Even though OCD is classified

as an anxiety disorder, the fifth edition of the Diagnostic and Statistical Manual (DSM-V) has separated OCD from other anxiety disorders, and it appears as one of several disorders which prominent features are obsessive preoccupation and repetitive behaviors.[12] Studies correlating anxiety disorders and OCD found that even though OCD and some anxiety disorders (Alexithymia and Anxiety Sensitivity) share some symptoms, OCD does not follow the classical model (traumatic event leads to conditioned anxiety or behavior) and additionally, anxiety seems to be controlled by a stronger correlation of emotion-aversion and symptom manifestation.[13,14] The diagnosis of OCD is given by the Yale-Brown Obsessive Compulsive Scale (Y-BOCS), a questionnaire that assesses the symptoms associated with OCD and gives a score, which is indicative of the severity of the condition.[4]

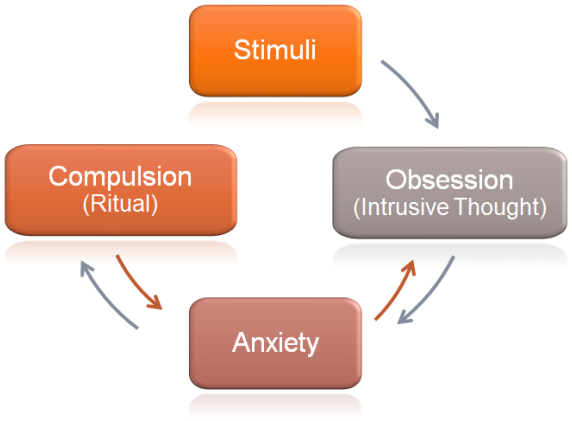

Figure 1. Schematic of steps involved in OCD. Performing the compulsion can decrease anxiety, but this results in reinforcing the obsession-compulsion loop through classical conditioning. Paradoxically, performing the ritual can cause anxiety to the individual.

1.2. Pathophysiology of OCD

Statistics reveal that, in the United States, approximately 5 million Americans (approximately 2.3% of the total population) are affected by OCD at one point in their lives,[4] and the World Health Organization (WHO) has classified OCD as the fourth major mental illness with significant morbidity.[6] As previously mentioned, OCD is a detrimental disease that significantly

decreases the quality of life of the individual. In a recent study, people with OCD reported having a lower quality of life than individuals with schizophrenia.[5] The current obstacle in the treatment of OCD is that there is no effective medication yet and the underlying neurological mechanism is not well understood.

1.2.1. Neuroimaging Studies (Brain Regions Affected by OCD)

Neuroimaging studies reveal the areas of the brain and the circuitry that is affected in OCD. Overall, these studies show a comparison between a healthy individual and an individual with the disorder. Additionally, it is possible to observe improvements in the brain under a specific treatment or medication. Through nuclear magnetic resonance imaging (MRI) studies, OCD patients have consistently indicated an anomaly in the orbitofrontal cortex (OFC), anterior cingulate cortex (AAC), basal ganglia, and thalamus.[4,6] From the previously mentioned areas, the most important region is considered to be the basal ganglia, due to its close relation with the glutamatergic transmission and its direct feedback (communication) with the thalamus and cerebral cortex; lesions to the basal ganglia have been reported to produce OCD.[4] In conjunction with the basal ganglia, MRI studies have also reported hyperactivity in the anterior circulate cortex (ACC), striatum, and orbitofrontal cortex (OFC).[56,62,97] Positron emission tomography (PET) and other neuroimaging studies (Such as: H^1MRI) reveal a relationship between levels of the neurochemical metabolites and dysregulation of the aforementioned regions; studies have consistently shown a dysregulation in glutamate/glutamine concentration in the OFC (higher), striatum (higher), ACC (lower), and left caudate cortex (lower).[30,56,63] Another study that corroborates the importance of glutamate/glutamine in OCD is the quantification of neurotransmitters in the cerebrospinal fluid, a study that reveals a correlation between symptom

severity and an elevated level of glutamate and glycine in the cerebrospinal fluid of OCD patients.[3,56] Other incidents that provide further evidence of the areas of the brain affected by OCD are focal brain injuries: people who had strokes affecting the inferior parietal, basal ganglia, caudate, and/or posterior frontal lobe have acutely shown OCD symptoms.[7,4,15] The relationship between the areas of the brain being overstimulated and the dysregulation of neurotransmitters led to the current model of OCD, which emphasizes the aberrant cortico - striato - thalamo - cortical (CSTC) modulation,[16,5,6,17] from which glutamate is the major excitatory neurotransmitter,[14,18] and which is also known to interact extensively with serotonin, gama-aminobutyric acid (GABA), and dopamine.[6]

1.2.2. Genetic Studies of OCD

Although the neurobiology and etiology of OCD is not fully understood, there are studies that suggest that this disease has a genetic basis, which predisposes certain individuals to develop OCD. Hereditary studies do not provide a concise genetic anomaly that can be correlated to the disease, but rather give an indication of a mutated gene that can be passed on to generations. In addition, it also proves that the disease is not exclusively a result of environmental factors: hereditary studies reveal that monozygotic twins have a higher probability (80–87%) for both to develop to OCD, in comparison to that of dizygotic twins (47–50%).[5,17] Development of this disease could also be explained through epigenetics, in which it is believed that through DNA methylation or other DNA modification mechanisms that can be influenced by environmental stimuli, some changes can occur, which can influence gene expression.

There have been several genome association studies, most of which are able to locate some relevant genes, but they are not able to consolidate their data with other results, or the data does not reach a very significant trend to be a concise association. We are only going to focus on the most relevant genes for the case study. Some of the genes associated with the glutamate neurotransmission system include the $SLC1_{A1}$,[19,4,6,20,21,17] which is a gene that encodes the Excitatory Amino Acid Transporter (EAAT)1/3, and is located on the post-synaptic and peri-synaptic membrane. This transporter is highly expressed in the cerebral cortex, striatum, and thalamus.[17] Another glutamate transporter gene associated with OCD is the $SLC1_{A2}$ gene, which encodes the EAAT2 glutamate transporter.[19,22,17] Both of these glutamate transporters maintain the glutamate concentration within normal range. The final glutamate-related genes are the GRIK2 (which codes for a kainate receptor subunit) and GRIN2B (which codes for the NR2B subunit of N-methyl-D-aspartate (NMDA) receptors).[23,22,17] Some genes associated with dopaminergic transmission include SLC6A3, which codes for a dopamine active transporter protein (DAT1) and its function is to provide dopamine clearance from the pre-synaptic cleft; DRD3, which codes for the dopamine receptor D3, which has been associated with schizophrenia and Parkinson's disease;[22,17] and two serotonin-related genes: 5-HTTLPR (also known as SLC6A4), which codes for a serotonin transporter that helps in the serotonin clearance, and 5-HTR_{2A}, which codes for a serotonin receptor that is associated with excitation, behavioral effects, learning, and anxiety.[4,6,22,24]

1.2.3. Genetic Animal Models in OCD

Animal models provide an insight to the probable molecular and genetic mechanism of the disease; additionally, they can help us test and tailor new drugs for the disease being

analyzed. The D1CT-7 (Ticci mouse) was among the first animal models of OCD: a model that correlates to the dopamine genetic abnormalities found in humans. This mouse expresses an intracellular form of cholera toxin that leads to a chronic potentiation of the D1+ neurons, which in turn produces an over-activation of glutamatergic output in the striatum.[25] The brain regions in which the cholera toxin transgene is expressed in DICT-7 mutant mice overlap with the neural circuitry implicated in OCD.[25] These mice, in addition to exhibiting OCD (compulsive grooming), also exhibit Tourette Syndrome (TS)-like behaviors (tics). Treatment with clonidine is shown to decrease tics, but not OCD symptoms. This mouse model would be most appropriate for the comorbid condition of OCD –TS, rather than just OCD.

The animal model that correlates to the glutamate system in OCD is the DLGAP3 (SAPAP3) Knockout mice. This model exhibits excessive grooming, and has defects in glutamatergic transmission at cortico-striatal synapses, which could be related to an abnormal NMDA receptor subunit NR1 (GRIN1), NR2B (GRIN2B) and NR2A (GRIN2A) composition, found in the post-synaptic density of striatal neurons. The use of a lentiviral vector reduced OCD-like behaviors.[22,25,17] The treatment with fluoxetine, a selective serotonin reuptake inhibitor (SSRI) reduces the grooming behavior in mice.[4,5,25] The problem with this model is that there is no consistent association across SNP studies in humans.[17]

The final animal model presented here is the SLITRK5 Knockout. This model also exhibits excessive grooming and anxiety behaviors; additionally, this mouse model has impaired cortico-striatial circuitry and abnormal glutamate activity. The SLITRK5 Knockout mice share some similarities with DLGAP3 (SAPAP3) Knockout mice, in which both exhibit an increase in

orbitofrontal cortex activity, and report changes in NMDA subunit composition, as well as glutamate receptor composition.[22,17] Treatment with fluoxetine reduces the OCD behaviors in this mouse model, just like in the previous model.[22]

There are other animal models; however, they were excluded due to the lack of evidence in correlation to OCD. Although they might have displayed OCD-like symptoms, they might have exhibited other comorbid conditions, or more work is required to establish predictive validity. Examples of these models include dopamine transporter knockdown (DAT KD) mice, which might be more suitable to study in TS with comorbidity with OCD due to the syntactic grooming they displayed.[25] Another example is the 5-HT2C Knockout mice, which might be more suitable for anxiety models due to the inconsistent anxiety behaviors displayed.[25]

1.2.4. Other Correlations with OCD Development

In addition to genetic and environmental factors (epigenetics), there are other factors that can be associated with the onset of OCD. One theory associates the pathogenesis of OCD to an autoimmune response triggered by a streptococcal infection. This condition is known as Pediatric Autoimmune Neuropsychiatric Disorders Associated with Streptococcal Infections (PANDAS), and the population that is at risk of this phenomenon is between the ages of 3 to 14. PANDAS is thought to originate through Group A beta-hemolytic streptococcal infections; via a phenomenon known as molecular mimicry, the antibodies mistakenly recognize and "attack" the basal ganglia, a mechanism similar to the cardiac effects produced from rheumatic fever. The antibodies have not been definitely identified yet.[4,26,27,17] Children with OCD derived from

PANDAS might have additional symptoms such as anxiety, urinary urgency, oppositional defiant disorder, and mood swings, in comparison with a patient with OCD only.[4]

There is also some evidence suggesting that nitric oxide (NO) might be an important element in OCD, since some studies found that OCD patients have higher NO levels than healthy individuals, and that these levels are positively correlated with the severity of OCD symptoms.[7] The evidence is supported by a decrease in NO levels as the OCD patients receive SSRI, anti-dopaminergic drugs, and the NMDA antagonist memantine.[7] However, this correlation could be consequence of the glutamate–nitric oxide–cGMP pathway, where the activation of an ionotropic glutamate receptor such as kainate, AMPA, or the NMDA receptor (previously proven to have SNP in humans), leads to increased calcium in the post-synaptic neuron, which in turn binds to calmodulin and activates neuronal nitric oxide synthase (nNOS).[28] In this case, NOS might be a side effect of the glutamate dysregulation in OCD.

Another phenomenon that can be related to OCD consists of reports that the female hormonal cycle might trigger or exacerbate OCD symptoms, as gonadotropine-releasing hormone (GnRH) agonists were reported to ameliorate OCD symptoms.[7] Other hormones that are correlated to the severity of the symptoms of OCD include vasopressin, oxytocin, and adrenocorticotropin; however, their influence on the severity of the symptoms is not fully understood.[7]

1.2.5. Pharmacological Drugs that can cause OCD-like symptoms

The molecular mechanism of the drugs that can cause or exacerbate OCD may provide a deeper insight of the neural pathways by which this disease functions. Recreational drugs that

produce OCD-like symptoms are: amphetamines, methylphenidate, meta-chlorophenylpiperazine (ecstasy), and cocaine.[4] Methylphenidate and cocaine act as dopamine-norepinephrine reuptake inhibitors; by binding to these transporters, they increase the dopamine and norepinephrine levels in the synaptic space. Amphetamines also increase the levels of dopamine and norepinephrine in the brain, although its mechanism of action is through their effects on monoamine transporters. Additionally, amphetamines also inhibit SLC1A1 genetic activity. In regard to ecstasy, its mechanism of action is as an agonist of serotonin receptors; the strongest binding happens at the 5-HT2B and 5-HT2C transporters, and it has been reported to exacerbate OCD in patients who have consumed.[4]

Prescription medications that produce OCD-like symptoms include ropinirole, pramipexole, and pergolide, which are dopamine agonists, especially of the D3 receptor.[4] Topiramate has also been reported to induce obsessive–compulsive symptoms;[17] however, the mechanism is not fully understood. Although not a prescription drug, arginine, which can be obtained as a supplement, has been linked to exacerbation of OCD; this may be related to the fact that arginine is a NO agonist and precursor that elevates the level of nitrides, and increases marble-burying behavior in mice.[7]

Some drugs that have induced OCD in mice include 8-hydroxy-2-di-n-propylamino-tetralin hydrobromide (8-OHDPAT) and quinpirole.[7] The case of 8-OHDPAT has become an animal model for OCD; upon administration of 8-OHDPAT (5-HT1A agonist), mice decrease spontaneous alternation (natural tendency of rats to explore novel places). The disadvantage of this model is that an acute administration of the drug is required for the model to have face validity; however,

it does seem to decrease OCD symptoms when supported by the administration of a serotonin reuptake inhibitor, as will be discussed later. Chronic administration of quinprinole (D2/D3 agonist)[27] can induce compulsive checking and ritual-like motor acts in rats. This OCD-like behavior is decreased by the administration of serotonin reuptake inhibitors, giving this model face validity.[19]

1.3. Treatment Options

As with most neurological disorders, there is a wide range of treatment options for patients with OCD. The first line of treatment approved by the FDA is the use of selective serotonin reuptake inhibitors (SSRI).[7,27] Additionally, the American Psychiatric Association recommends that individuals engage in cognitive behavioral therapy (CBT) focusing on exposure and response prevention therapy. The problem with OCD is that due to the complexity of this disorder, about 50% of the patients do not respond to current pharmacological medications,[29,30] and patients who do respond to the pharmacological interventions might not feel a complete relief of the symptoms.[18,5,15] The treatment paradigm for most OCD medications is to begin with a low dose and increase gradually. The disadvantage of this is the myriad of side effects a patient can experience. It is also recommended, once the individual starts with a treatment, to follow up for at least three months, since most of the medications do not provide immediate symptom relief.[31] It is also important to mention that, even though anxiety is a big component of the disease, anxiolytic drugs are not effective in alleviating obsessions and compulsions.[7]

The most accepted method to measure OCD in humans is the Yale-Brown Obsessive Compulsive Scale (Y-BOCS),[32,27] a rating scale intended to be used as a semi-structure interview.

The interview assesses and rates the severity and type of symptoms with respect to time spent, interference, distress, resistance, and control in patients with Obsessive Compulsive Disorder (OCD).[32] The obsessions and compulsions are rated in a scale from 0 to 4, where zero is classified as none and four is classified as extreme or incapacitating. The array of questions in this rating system has shown internal consistency and validity for patients with OCD. The Y-BOCS test can be viewed at the appendix section of this proposal. Most of the studies presented in this proposal measure symptom reduction by Y-BOCS, with the exception of animal models, for they have a different paradigm to measure OCD symptoms. To better understand the treatment options used in OCD patients, the treatments are going to be divided in pharmacological treatment, alternative medicine, psychological treatments, and surgical interventions.

1.3.1. Pharmacological Treatments

Pharmacological treatments refer to the drugs that have a synthetic origin. The most popular medications for OCD are the SRI; however, there are other medications that target ionotropic, glutamatergic, and norepinephrine receptors. Experimental treatments for OCD are based on the neural circuitry being affected by OCD.

1.3.1.1. Serotonin Reuptake Inhibitors

Selective serotonin reuptake inhibitors (SSRI) and serotonin reuptake inhibitors (SRI) are drugs that block the reuptake of serotonin (by binding to a transporter protein); as a result, there is an increase in the serotonin levels in the pre-synaptic cleft. SSRIs are designed with a specific biological target, compared to SRI, which do not really have a specific biological target, and thus can bind to other transporters. SSRI are the first line of treatment for OCD. These medications

are usually prescribed as antidepressants; however, they seem to alleviate the symptoms of OCD. The most probable mechanism of action of SRI drugs might be through inhibition of glutamatergic transmission in the orbitofrontal cortex.[5,15] As previously stated, individuals with OCD display excessive baseline activity of excitatory glutamatergic neurons; therefore it is hypothesized that the increase in serotonin levels will ameliorate glutamatergic transmission, resulting in symptom reduction, although there is no definitive mechanism as to how this occurs.

Most commonly, a patient with OCD will try two to three drugs before finding the one that works best for them.[1] The most common side effects associated with SSRI and SRI are dry mouth, sweating, constipation, drowsiness, tremor, sexual side-effects, weight gain, nausea, sleeplessness, and headaches; rare cases include manic episodes and seizures.[1] As previously stated, not all OCD patients respond well to SRI or SSRI; however, for patients who are resistant to SRI treatment, another drug is added in an attempt to increase effectiveness. This is known as "augmentation therapy," which consists on the addition of serotonin reuptake inhibitors, typical and atypical antipsychotic drugs, glutamatergic agents, or natural remedies.[1] Safe and approved methods of augmentation therapy include psychological treatments like CBT. Table 2 illustrates and describes the SSRI and SRI that have been used in the treatment of OCD.

Table 2. Brief description of the SRI and SSRI medications used for the treatment of OCD. The commercial name of the compounds is given in parenthesis.

Serotonin Reuptake Inhibitors		
Drug Name	Data	Structure
Clomipramine* (Anafranil)	Clomipramine is the oldest and best studied of the SRI medications. It is a highly selective inhibitor of serotonin reuptake (5-HTT). Usually prescribed when other SSRI treatments are not effective. Although clomipramine may be slightly more effective than other SSRI, it is usually not prescribed because there are more adverse side effects, among which is the potential for cardiac toxicity, including QTc prolongation.[1,4,33]	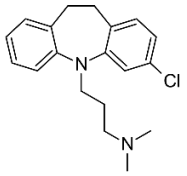
Fluvoxamine* (Luvox)	Fluvoxamine demonstrated similar efficacy but superior tolerability over clomipramine. Fluvoxamine, in addition to functioning as an SSRI, also works as a σ1 receptor agonist (trans-membrane ER chaperon protein that is linked to depression).[4,1]	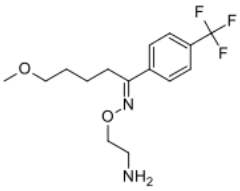
Fluoxetine* (Prozac)	Fluoxetine interacts with cytochrome P-450 (CYP) 2D6 to produce its active metabolite norfluoxetine. This drug has a weaker binding that fluvoxamine.[4]	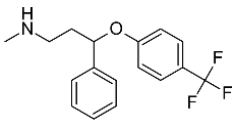

Paroxetine* (Paxil)	Paroxetine is one of the most potent and selective SSRI; additionally, it inhibits the reuptake of norepinephrine more than other SSRI. Paroxetine is more likely to cause birth defects and has category D rating from the FDA.[4,6]	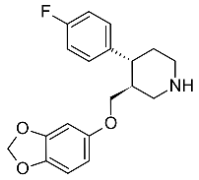
Sertraline* (Zoloft)	In addition to being an SSRI, sertraline inhibits the reuptake of dopamine more than the other SSRI. Sertraline tends to be associated with a higher rate of psychiatric side effects.[4]	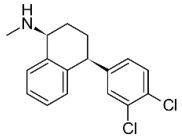
Escitalopram (Lexapro)	Escitalopram is the S-enantiomer of citalopram. There have been studies that demonstrate the efficacy in the treatment of OCD; however, this SSRI does not have FDA approval for treating OCD.[4] The main use of this drug is to treat major depression disorders.	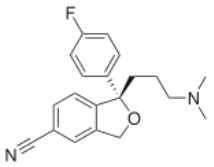
Citalopram (Celexa)	Citalopram is an SSRI that, like escitalopram, can function for the treatment of OCD, but is not approved by the FDA for that purpose.[4] One of the most important side effects of citalopram and escitalopram is a QTc prolongation, especially in overdose.	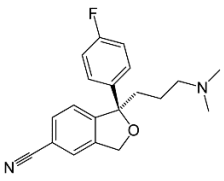

**FDA approved to treat OCD. Additionally, have received highest category of evidence to treat OCD, according to the Guidelines of the World Federation of Societies of Biological Psychiatry (WFSBP). [4,1,3]*

1.3.1.2. Ionotropic Glutamate Receptors

These medications are not approved by the FDA for the treatment of OCD; however, due to genetic evidence in single nucleotide polymorphism (Grin2B, [codes for NMDA subunit] and

GRIK2/GRIK3 [codes for a kainate subunit]) and key neuro-metabolites (glutamate)), it appears that there might be a connection between the ionotropic receptors and OCD. Studies have favored the NMDA receptors because they have the highest affinity for glutamate (EC50 1 µM);[20] additionally, they have been linked to anti-compulsive effects in animal models of OCD.[34] The other ionotropic glutamate receptors which also have potential for OCD target medication are the kainate (KA) receptor and α-amino-3-hydroxy-5-methyl-4-isoxazole proprionic acid (AMPA) receptor. These three ionotropic receptors are activated by glutamate and mediate most of the rapid synaptic excitation throughout most of the vertebrate central nervous system.[35] Furthermore, some of these medications can be used as augmentation therapy to enhance the effects of the SSRI.[4] Table 3 provides more information about the medicine targeted at ionotropic receptors for the treatment of OCD.

Table 3. Brief description of the medications used in OCD that target ionotropic receptors. The commercial name of the compounds is given in parenthesis.

Pharmacological Treatments Involving Ionotropic Glutamate Receptors		
Drug Name	Data	Structure
D-cycloserine (Seromycin)	D-cycloserine is a partial NMDA agonist that has had mixed results in OCD patients. While some patients report an improvement in conjunction with cognitive behavioral treatment (taken one hour before session),[17] other studies report that the data is not significantly different.[6] It has also been reported that D-cycloserine-treated rats display decreased compulsive lever pressing.[17]	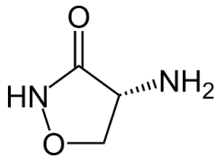

Dizocilpine (MK-801)	Dizocilpine is a potent NMDA receptor antagonist (channel blocker).[36] In mice, Dizocilpine showed no effect on lever pressing experiments, but mice from another study decreased marble-burying behavior; however, these mice displayed an increased locomotion in comparison to the control.[4] Additionally, it has been shown that this drug has antidepressant-like effects.[37]	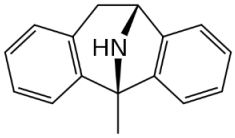
Memantine	Memantine is a non-competitive NMDA receptor antagonist.[4] It has shown efficacy as an augmentation agent in refractory OCD in several case reports.[17] Memantine has also received FDA approval for the treatment of Alzheimer's disease.	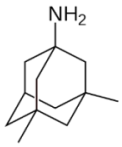
Amantadine	Amantadine is an NMDA receptor antagonist. It has reduced marble-burying behavior in mice, with greater effectiveness compared to memantine and riluzole.[6,17]	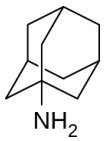
Ketamine	Ketamine is an NMDA receptor antagonist. Studies have revealed that it has anti-OCD properties.[37] It has also shown antidepressant effects in OCD patients with comorbid depression.[37]	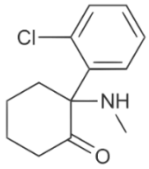
NBQX	NBQX is an AMPA receptor antagonist. Administration of this drug showed no effect on marble-burying behavior in	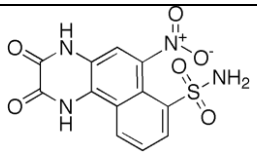

	mice,[7] demonstrating the importance on NMDA receptor activity in OCD.	
Riluzole (Rilutek)	Riluzole has been reported to inhibit the kainate and NMDA receptors. It is also a glutamate antagonist (release inhibitor) and stimulates glutamate uptake by astrocytes. Its mechanism of action has not been fully elucidated. Riluzole was found to be effective for children with OCD, and as an augmentation agent for patients who are SRI-resistant. However, riluzole showed no effect on marble-burying behavior in mice, which could have been because the model lacked face validity on inducing the OCD symptoms.[7,6,17]	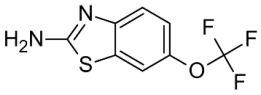

1.3.1.3. Antipsychotics

Antipsychotics can be divided in two categories: typical (refers to the first-generation antipsychotics) and atypical (second-generation antipsychotics, which also act on serotonin receptors). Most of these drugs are for patients who suffer from schizophrenia or bipolar disorder. Antipsychotic treatment is only given to patients whose OCD is SRI-resistant. This treatment targets dopaminergic and serotonergic loops as receptor agonists.[17] The use of antipsychotics for the treatment of OCD began as one study reported an improvement of OCD symptoms with the use of haloperidol as augmentation therapy with fluvoxamine; it is hypothesized that the dopamine (D2) receptors might play a role in the attenuation of the OCD

symptoms.[5] The main problem with this medication is the adverse side effects. Most antipsychotics are used as augmentation therapy, and in some instances they may exacerbate OCD symptoms.[4] It is difficult to assess which antipsychotic is effective as augmentation therapy, as some studies may show opposite results; such is the case of clozapine, which is reported to induce, aggravate, and alleviate OCD symptoms.[33] Table 4 gives a brief overview of the antipsychotic medications used in the treatment of OCD. Perhaps the limited efficacy of these drugs is due to their ability to act on certain serotonin receptors as agonists; however, a complication arises when the drugs act on dopaminergic receptors as well.

Table 4. Brief description of the antipsychotic medications used to treat OCD. The commercial name of the compounds is given in parenthesis.

Pharmacological Treatments Involving Antipsychotics		
Drug	Data	Structure
a) Clozapine (Clozaril1) b) Quetiapine (Seroquel1) c) Olanzapine (Zyprexa) d) Ziprasidone (Geodon1)	These six drugs are atypical antipsychotics. The majority of the studies, except for a few with small sample sizes[38] (shown below), reveal that none of these drugs are effective in treating OCD.[4,17] Olanzapine augmentation with SSRI has been reported to be as successful as risperidone.[6] In a 12-week, open label trial of aripiprazole, significant improvement of OCD symptoms was demonstrated[6]	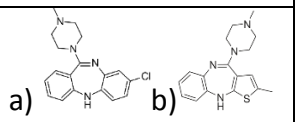 a) b) 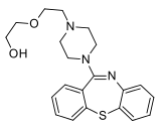 c) 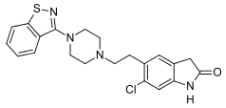 d) 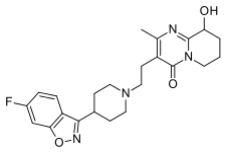 e) 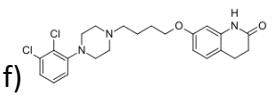 f)

e) Paliperidone (Invega) f) Aripiprazole (Abilify1)	A study found that clozapine down-regulates the protein produced by SLC1A1 (EAAC1/3) in the cingulate cortex of the rat,[17] supporting the existence of a relationship between glutamate in the synaptic cleft and OCD. There are also reports that these drugs, except for ziprasidone, can cause OCD in other patients who do not have it.[4,39]	
Risperidone (Risperdal)	Risperidone is a more potent serotonin antagonist compared to dopamine antgonist. This atypical antipsychotic has been tested in OCD with limited benefit.[4,1,6]	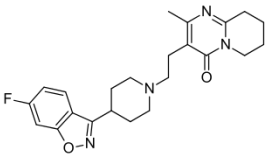
Haloperidol (Haldol)	Haloperidol is an antipsychotic medication that is a D2 (dopamine) receptor agonist, as well as a serotonin agonist at a higher dose. When used as an augmentation treatment with SSRI, haloperidol reduces symptoms of OCD, particularly in patients with comorbid tics.[1,5]	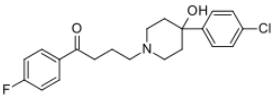
Pimozide (Orap)	Has a higher binding affinity than haloperidol, acting as a D2 receptor agonist. It has been reported to modestly reduce symptoms of OCD, when used in augmentation treatment with SSRI.[1]	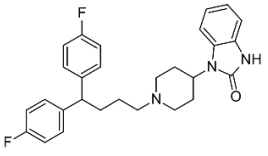

1.3.1.4. Other Pharmacological Interventions

This section refers to other drugs that have been tested as potential treatments for OCD. Most of them are used as augmentation therapy, and are not approved by the FDA to treat OCD; however, some seem to be effective for some patients. Table 5 provides data for these other pharmacological interventions that have been tested for the treatment of OCD.

Table 5. Brief description of the alternative pharmacological interventions that have been used to treat OCD. The commercial name of the compounds or abbreviation is given in parenthesis.

Alternatives to OCD Medications		
Drug	Data	Structure
L-tryptophan	L-tryptophan is essential for the body to produce serotonin. Based on the evidence that serotonin levels affect OCD, L-tryptophan seems like a good candidate for enhancing serotonergic transmission in the CNS. People who have tried L-tryptophan in combination with an SRI have had very limited benefit.[34,1]	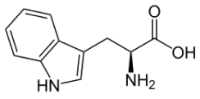
Inositol	Inositol is an isomer of glucose, and it was once considered to be part of the B vitamin complex.[34] Inositol has had mixed results in OCD treatment. Overall, studies suggest that for inositol to be effective, a high concentration[1,34] (more than 1,000 mg) must be prescribed, since a lower concentration does not produce significant results.[2]	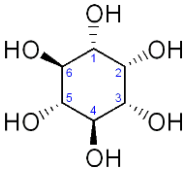

Lithium	Lithium is known for its use in bipolar disorder and depression. Augmentation therapy of lithium versus placebo found no benefit in lithium augmentation.[4,1]	----------
N-acetylcysteine	N-acetylcysteine (NAC) is a cysteine derivative that is less susceptible to oxidation, and more soluble in water than cysteine. NAC has been proposed as a treatment for OCD because it can inhibit synaptic glutamate release through the cysteine-glutamate exchange. When cysteine levels are increased, so is the extracellular glutamate in the extra-synaptic space, which in turn leads to stimulation of mGluR2/3 receptors and, as a consequence, inhibition of synaptic glutamate release.[38,6,67] NAC augmentation with fluvoxamine results in a significant improvement in OCD symptoms.[34,17]	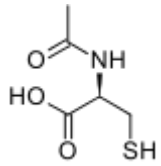
Serotonin – norepinephrine reuptake inhibitors (SNRI)	Although they inhibit serotonin in conjunction with norepinephrine, so far they have not yielded significant symptom improvement. Among the tested drugs are venlafaxine, duloxetine, milnacipran, and levomilnacipran.[4,39]	----------
Ondansetron (Zofran)	Ondansetron is a 5-HT3 (serotonin) receptor antagonist. When used as monotherapy in SRI-resistant OCD patients,	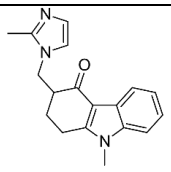

	it was reported that half of the patients in a small trial group presented symptom reduction.[4]	
Pregabalin	Pregabalin inhibits glutamate release via blockade of calcium channels. Beneficial effects on OCD symptoms in combination with SSRI have been reported.[6]	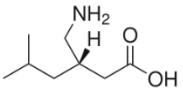
Dronabinol (THC)	Two case reports showed Improvement in refractory OCD with the cannabinoid Dronabinol.[6]	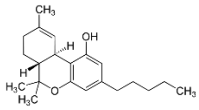
Monoamine Oxidase Inhibitors (MAOI)	The MAOI have a history of being used for depression. The disadvantage is that they inhibit the oxidation of monoamines, which can bring upon a myriad of side effects; in addition, they can also create some dependence. Phenelzine (Nardil) and tranylcipramine (Parnate) are MAOI that have been used to treat OCD, and were reported to have limited benefits, being less effective than SRI medications.[1]	----------
Morphine	Morphine has shown efficacy in treatment-resistant OCD. The mechanism is not fully understood, but it is thought to act by inhibiting glutamate release through disinhibition of serotonergic neurons.[6]	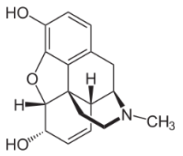

1.3.2. Alternative Medicine Treatments

Alternative medicine can elicit fewer side effects than typical pharmacological medication. Most of the time, alternative medicine is used as augmentation therapy or as a supplement to ameliorate the severity of the symptoms. Most of the alternative medicines are based on herbal medicine, and are taken as infusions or as food supplements. Approximately 44% of patients hospitalized for acute care of various psychiatric disorders have used herbal medicine to ameliorate their illness.[32] The problem with some of these remedies is that some phytochemicals may interact with prescription medicine in a negative way, which may reduce the potency of the medication. One of the main obstacles of herbal medicine studies is that the dosage of the phytochemicals cannot be accurately assessed.

Table 6. Brief description of the alternative natural medications used to treat OCD. The common name is given in parenthesis.

Herbal Medicine	Data
Hypericum perforatum (St. Johns worth)	A well-known plant used for the treatment of depression and anxiety. It is believed to increase binding sensitivity to 5HT1A receptor and inhibit neuronal release of glutamate. The mayor constituents are hyperforin and hypericin. No significant results have occurred against OCD symptoms.[40,41,42]
Silybum marianum (Milk thistle)	It is commonly used as a hepato-protective agent. In preclinical studies it has been found to increase serotonin levels in the cortex. It has been shown to reduce symptoms of OCD.[34] The mayor phytochemical is the flavonoid complex known as silymarin.

Methanolic extract of *Benincasa hispida* fruit (winter watermelon)	Traditionally used to increase appetite. It exhibits significant anti-compulsive effects in marble-burying behavior tests in mice, and the effect may be attributed to an enhanced serotonergic function. Its effects are comparable to fluoxetine.[43]
Echium amoenum (Borage)	Used in traditional Iranian medicine as an anxiolytic. A study shows that it significantly reduces OCD and anxiety. [23,44] In addition, animal models have revealed borage as having anxiolytic and sedative effects comparable to diazepam.[21]
Lagenaria siceraria (Calabash)	This food item has shown to attenuate OCD in marble-burying behavior.[21]

Doctors in the field of homeopathic medicine suggest to avoid chorine, dimethylaminoethanol, copper, or folic acid supplements, because they often exacerbate OCD symptoms,[22] but advise to take methionine, s-adenosyl methionine, calcium, magnesium, B-6, inositol, betaine anhydrous, and zinc supplements, because they help in the treatment of OCD.[2] Other alternative methods include acupuncture, mindfulness meditation, yoga breath work, progressive muscle relaxation, and meridian tapping.[21]

1.3.3. Psychological Treatments

The recommended psychological treatment for people with OCD is cognitive behavior therapy (CBT) focused in exposure and response prevention therapy. In this approach, the patients are exposed to the anxiety-provoking stimulus, and the therapist encourages the patient to avoid the use of compulsions in order to foster habituation. The goal of this treatment is to teach the patients with OCD to be less anxious around the stimulus, and avoid performing rituals. For this treatment to be effective, 10 to 20 hours of therapy are necessary to achieve favorable outcomes. This particular treatment has a success rate as high as 80 percent in the reduction of the symptoms.[32,11,33] Due to the success of this therapy, it is considered the psychological treatment of choice for OCD.[32] CBT can be performed as an individual therapy or as a group therapy. Studies have found small difference between the individual versus the group therapy. The downside of psychological treatments is that success of the therapy is dependent on the experience of the therapist, and the commitment of the patient to the treatment. For patients who are using this therapy as augmentation, it is recommended to avoid benzodiazepine drugs (anxiolytic) because they affect short-term memory and learning.[1,33]

1.3.4. Surgical Interventions

These surgical interventions are uncommon, and are only performed where affected OCD patients have exhausted conventional therapies. These operations target the cortico-striato-thalamic-cortex (main brain circuitry in OCD).[54,6] One of the surgeries performed is the anterior cingulotomy, which involves a lesion on the anterior cingulated cortex and cingulum.[6,15] Another neurosurgical procedure is deep brain stimulation, which consists on implanting a pacemaker to send electrical impulses, which stimulate a specific area of the brain; in the case of

OCD, stimulation is given to the internal capsule and/or the adjacent ventral striatal region, which may be effective for severely affected OCD patients.[6]

1.4. Summary of OCD

OCD is a complex mental disorder, and its pathology has not been fully elucidated. People who suffer from this disorder experience an obsession and, to alleviate the stress associated, they perform a compulsion, which can be characteristic to every individual. The current treatment options are not effective for all patients, and most of the treatments carry unwanted side effects. Through the neuroimaging studies, experts in the field have derived a model that correlates important neurotransmitters with parts of the brain that are involved in the disorder. Through genetic studies, we can correlate specific proteins and link them to the disorder protein, such as NMDA receptor, kainate receptor, EAAT 1/3, as well as serotonin receptors, and dopamine transporter D3. As for pharmacological interventions, we can deduce that blocking dopamine receptor D1 can exacerbate the symptoms; however, for dopamine receptor D2, the drugs had limited effect and the results are inconclusive. In regard to psychological treatment, CBT yields good results and can be used as an augmentation therapy for the patients. The other treatment options deal with traditional medicine and can yield good results; however, more research is needed to better elucidate the bioactive components of these remedies.

Through the amount of evidence obtained from OCD in correlation to the areas of the brain being affected, there is a proposed glutamate dysfunction model. This model makes use of the CSTC circuitry and it is represented in figure 2. In short, there are two pathways by which signal transduction occurs in the CSTC circuitry. The first pathway is called the direct pathway; in

it, the striatum sends an inhibitory GABA signal to the globus pallidus interna, which in turn decreases inhibitory action in the thalamus and, as a result, there is an excitatory glutamate signal sent from the thalamus to the OFC and AAC. In the second pathway (indirect), the striatum sends and inhibitory GABA signal to the globus pallidus externa, which decreases its inhibition to the subthalamic nucleolus (STN) and, as a result, the STN sends an excitatory glutamate signal to the GPi, which in turn inhibits the thalamus. According to the OCD dysfunction model, there is an overstimulation of the direct pathway, which in turn leads to glutamatergic overstimulation in the AAC and OFC.

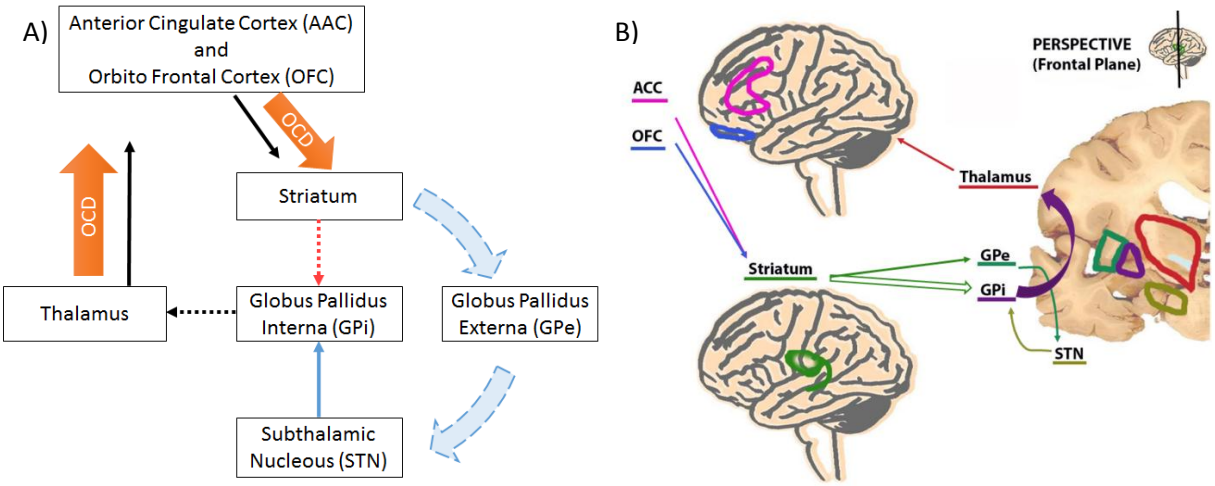

Figure 2. Illustration of a simplified diagram of the Cortical Striatal Thalamic Cortical (CSTC) circuit. A) Dashed lines represent GABA neurotransmission, and solid lines represent glutamate neurotransmission. Red arrows represent the direct pathway and blue arrows represent the indirect pathway. Orange arrows represent the dysfunction or areas being overstimulated by patients with OCD. B) Brain areas of the CSTC circuit.

1.5. Excitatory Amino Acid Transporter (EAAT) and OCD

Understanding the neurochemistry of OCD is central for the advancement of more effective medication, and as presented previously there seems to be a strong correlation between OCD and glutamate. Experimental evidence indicates that, by blocking or decreasing

NMDA receptor function, an improvement in OCD symptoms is observed. However, blocking NMDA receptor activity can produce severe side effects. Decrease in NMDA receptor activity can also be elicited by decreasing glutamate in the synaptic cleft via stimulating EAAT3.

The EAAT protein family belongs to the solute carrier 1 transporter family and it is responsible for glutamate transport in different parts of the body, this family of transporters exhibit up to 60% amino acid sequence identity with each other.[45,46] EAAT1 and EAAT2 are found predominantly in glial cells on the brain. EAAT3 and EAAT4 are predominantly expressed in neurons. Finally EAAT5 is mostly found in the retina. We will focus on the EAAT3 protein because it is selectively enriched in the neurons of the hippocampus, basal ganglia, cerebellum, and olfactory bulb,[47,48] which are some of the areas implicated in OCD; thus, stimulating EAAT3 can lower extracellular glutamate concentrations in these areas and ameliorate the OCD symptoms. From the previously presented evidence, targeting the EAAT3 protein for the treatment of OCD seems to be a viable option. The mechanism of action of EAAT3 involves the initial binding of three Na^+ and one H^+ ions with glutamate or aspartate across the membrane while the transporter countertransports one K^+ ion (Figure 3).[47,49] It is believed that the EAAT3 proteins assemble in trimmers, with each unit functioning like a monomer.[49,50] This transporter is localized in the post-synaptic cleft of neurons but it is also found in the kidney, where it functions as glutamate/aspartate transporter. Loss of function of this transporter can result in dicarboxylic aminoaciduria.[46,50]

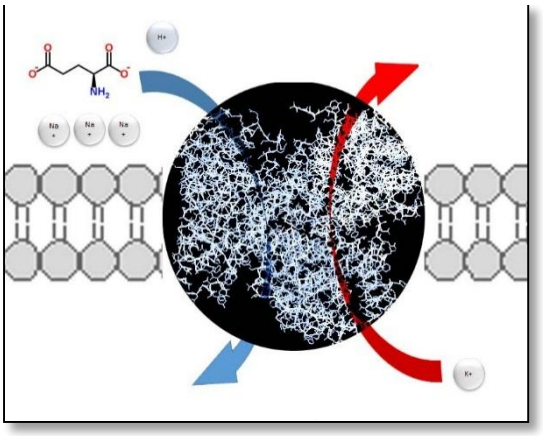

Figure 3. Blue arrow depicts the transport of glutamate, and the red arrow depicts the countertransport of potassium ions across the transporter.

To date, there is no crystal structure of the EAAT3 transporter; as a result, most computational studies utilize the crystal structure of the glutamate transporter homologue (GltPh), from *Pyrococcus horikoshii*, an archeal homolog that shares a 37% sequence identity with the EAAT family. Initially this might appear as a poor model to follow; however, the homology is much higher for residues near the binding pocket, reaching around 60% in this region.[11] Furthermore, almost all of the residues shown to be involved in the binding of the ions and glutamate in GltPh are conserved in the EAAT family. These computational calculations have yielded important information in regard to inhibitors and allosteric regulators for EAAT proteins.[8] Table 7 provides a list of the relevant molecules known to bind to the EAAT3 protein.

Table 7. Brief description of the EAAT3 substrates.

Substrate	Data	Structure
a) L-Glutamate b) L-Aspartate c) L-Cysteine	Gluatamate and aspartate are the endogenous ligands of the EAAT3 protein; however, it is also known that EAAT3 is able to transport the amino acid cysteine.[51,52]	a) 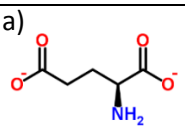 b) 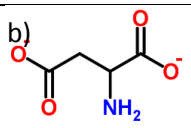 c) 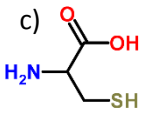

L-trans-2,4-pyrolidine dicarboxylate	L-trans-Pyrrolidine-2,4-dicarboxylic acid is a glutamate uptake blocker; it increases the extracellular glutamate levels in the synaptic cleft.[53]	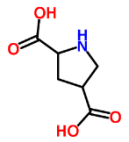
Clonidine	Clonidine reduces the response to L-glutamamte uptake in EAAT3 proteins.[47]	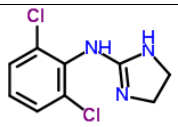
a) L-β-threo-benzyl-aspartate b) NBI-59159 c) DL-TBOA	L-β-threo-benzyl-aspartate, NBI-59159 and L-TBOA inhibit the neuronal EAATs.[54] L-β-threo-benzyl-aspartate is more specific for EAAT3 [54,55] DL-TBOA has proven to be an effective inhibitor, specially toward EAATs 2 and 3. This molecule has also been employed in radiolabel studies to find the binding affinity to the EAATs proteins.[56,57]	a)  c 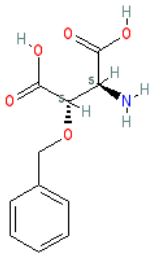 b) 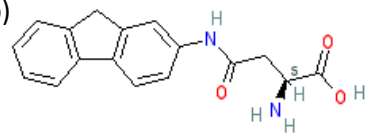
L-(-)-threo-b-hydroxyaspartate	L-(-)-threo-b-hydroxyaspartate is a substrate that resembles the endogenous activity of l-glutamate, in EAATs 2 and 3.[50]	

Threo-3-methylglutamate	Threo-3-methylglutamate is an EAAT2 inhibitor, but at higher doses it also inhibits EAATs 3 and 4.[50]	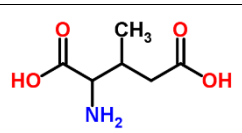
a) Lidocaine b) Isoflurane c) Propofol d) Benzodia-zepine	All of these molecules have been reported to increase EAAT3 activity.[27,58, 59]	a) 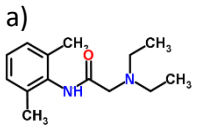 b) 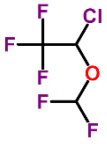 c) 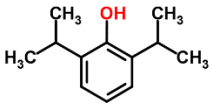 d) 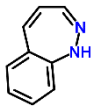

CHAPTER 2: SIGNIFICANCE AND INNOVATION

Up to date, the first line of medication against OCD is the use of selective serotonin reuptake inhibitors (SSRI); however, due to the limited success of SSRI, many patients remain significantly impaired by their symptoms. Even though the pathophysiology of OCD is not fully elucidated, there is a strong line of evidence correlating the excitatory neurotransmitter glutamate and the symptom severity of OCD. This theory is supported by genetic studies, neuroimaging studies, animal models, small clinical studies, and case reports presented in this proposal. As such, a novel therapeutic intervention targeting the glutamatergic pathway is needed. This proposal will focus on the dysregulation of the glutamatergic pathway in OCD via the EAAT3 protein.

The research strategy is to pharmacologically intervene EAAT3 by computational methods. This research changes the vision of the field, being that it is the first study to target the EAAT3 activity in OCD patients. Although there has been development of drugs to target these receptors, these drugs are used for anxiety disorders. This new approach aims to yield data that will improve the understanding of glutamate regulation in OCD. The results of this study will yield an improved understanding of the neurobiology and etiology of OCD.

2.1 Hypothesis

We hypothesize that stimulating the EAAT3 protein with lidocaine will produce a reduction in symptoms in OCD patients. The current OCD model emphasizes an aberrant glutamatergic system; stimulation of the EAAT3 protein through lidocaine could potentially decrease the excess glutamate in the synaptic space and, as a result, diminish OCD symptoms.

We will test our hypothesis by using in-silico docking calculations; in addition, we will identify drug candidates that will have a stronger docking affinity to the EAAT3 protein.

2.2 Specific Aims

The specific aims are subdivided in three parts: (1) Create molecular models of the EAAT3 protein structure. Once several models are obtained, a refinement process will be applied and the best models will be selected to identify potential binding sites. (2) Perform the docking of the hit compound (lidocaine), evaluate the contribution of molecular contacts, and test several parent compound constructs to further improve the molecular contacts of the binding pocket. We will strive to create *de novo* ligands for the protein-binding pocket. (3) Finally we will perform molecular dynamics calculations to assess the structural stability and find relevant motifs in the binding of the protein-ligand complex.

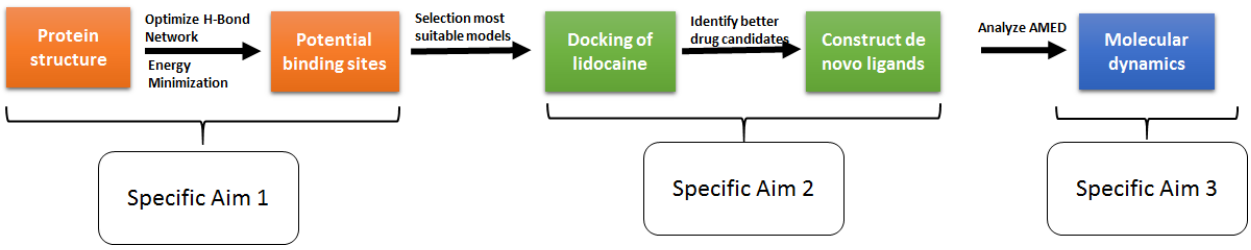

Figure 4. Schematic of the computational paradigm.

2.2.1. Specific Aim 1: Homology modeling of the EAAT3 protein structure and binding site identification.

Since there is no X-ray crystal structure, high resolution Cryo-EM, or high resolution NMR data of the EAAT3 protein, we will use the amino acid sequence of the protein (provided in supplemental material section) to construct the EAAT3 structure. The homology models were produced using the following software: I-TASSER (Iterative Threading ASSEmbly Refinement),

ModWeb, Phyre^2 (Protein Homology/analogY Recognition Engine V 2.0), SWISS-MODEL, and Schrödinger Maestro Academic Version. Even though each software has a different way of producing a protein model, they all follow similar steps: based on the sequence imputed, the software searches in a protein data base for proteins with similar sequences; thereafter, each software follows a particular algorithm to match the sequence homology to the current available structure. For more information about these algorithms, refer to supplemental material.

Once the protein models are completed, it is necessary to evaluate and refine the protein model structure. This step is crucial to optimize the hydrogen bond network and give the structure a low energy conformation. The first optimization will be performed using the Schrödinger Maestro protein preparation wizard, a program that will ensure structural accuracy by adding missing hydrogen atoms, resolving protonation states, revising bond orders, and optimizing the hydrogen bond network.[79] We then evaluate the protein models based on the following scores: QMEAN (the quality estimate ranges between 0 and 1, where higher values indicate better models), Z-SCORE (compares the model to reference structures solved by X-ray crystallography, where higher values indicate better models), and dDFIRE/dDFIRE2 (a distance-scale finite ideal-gas reference, an energy scoring function where the more negative the values, the better the model). These parameters allow us to assign a score to the protein model, which we can use to select the best model. The results of the model quality estimation are given in table 11 in the appendix section; additionally, the Ramachandran plot for each respective homology model is given. The Ramachandran plot provides an overview of allowed and disallowed regions of torsion angle values, serving as an important indicator of the quality of protein three-dimensional structures. It is important to note that quality estimates for membrane

proteins may receive very low Z-scores since their physico-chemical properties differ considerably from those of soluble proteins.[10]

Analyzing the data from the homology model studies, tables 12 and 13, we selected the best protein model from the different homology algorithms used. We then further processed the best scoring models through another refinement process using the 3Drefine protein structure refinement server. In this structure refinement, the hydrogen bond network is optimized and the energy of the model is minimized using the MESHI molecular modeling package.[12] Although the multimer homology models were not accepted by the server, the refinement process yielded five protein structures per each refined homology model. Table 8 displays the best scores resulting from the best protein models produced.

*Table 8. Further refinement of the best models from each structure homology model algorithm. *Depicts data from previous optimization data.*

Protein Model	**Best refined structure from 3Drefine server**	**QMEAN-Score**	**Z-Score (dDfire/dDFIRE2)**	**Ramachandran Plot**
Schrödinger structure 1 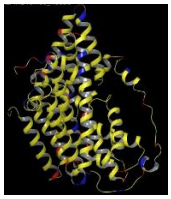	Model 5	0.484	-3.34 (-1092.37/ -808.077)	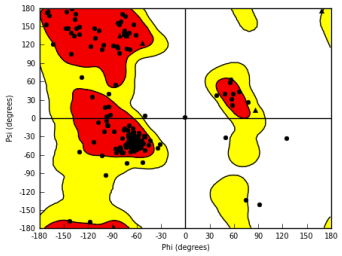
Schrödinger structure 4P19 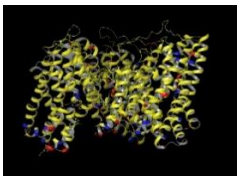	Structure could not be process	*0.635	*-1.332 (-3373.50 /-2601.08)	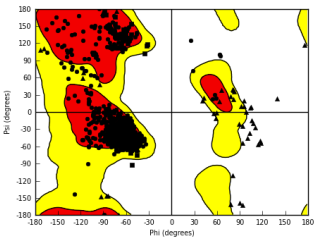

ITASSER structure 5 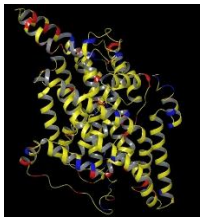	Model 5	0.536	-2.70 (-1277.53/ -977.031)	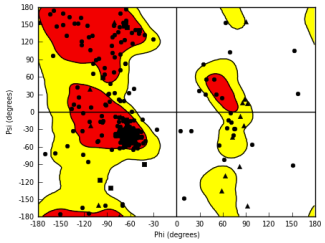
Modbasestructure2 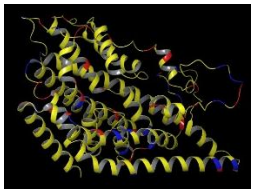	Model 3	0.478	-3.41 (-1078.35/ -813.615)	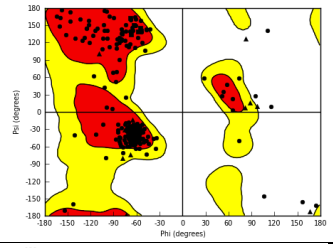
Phyre structure 1 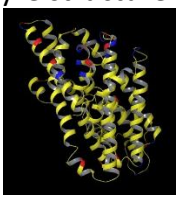	Model 4	0.466	-3.54 (-1090.97/ -806.912)	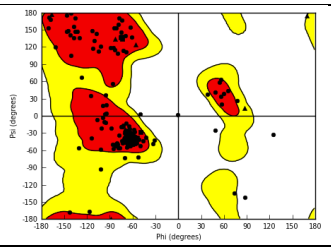
Swiss server structure 1 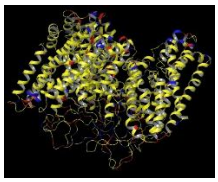	Structure could not be process	* 0.530	* -2.62 (-3206.86 /-2588.89)	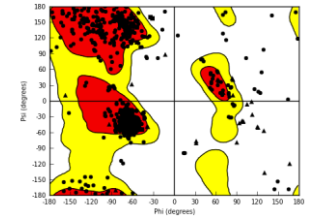

From the previous data we can conclude that the best multimeric unit is the Schrödinger model 4P19, and the best monomeric unit is the refined ITASSER model 5. For purpose of simplicity and to lower the burden of computational calculations, we will work with the monomeric units for the docking and molecular mechanics studies. Additionally, we will now refer to these models as “best” i.e. ITASSER structure 5 refinement model 5 will now be simply be called ITASSER best.

Now that we have our protein models we will proceed to identify possible docking sites on the protein structure, for this we used a server called Metapocket 2.0[69,70], which combines

the power of 8 binding site predictors: LIGSITE^{cs}, PASS, Q-SiteFinder, SURFNET, Fpocket, GHECOM, ConCavity and POCASA. This allows the user to have a bigger range in protein binding sites. The advantage of this server is that it calculates the z-score value for each protein binding site and, based on this information, it discards poor binding sites form each predictor; thereafter, it clusters the binding sites from the different predictors according to their spatial similarity. The output from the clusters will again be ranked by the total z-score values. In this particular study, we found several potential binding sites per each protein model; the data is provided in table 9.

Table 9. Results from the MetaPocket 2.0 binding prediction software.

Protein Model	Total Z-score /(Rank)	Coordinates
ITASSER Best	12.73 / (1)	X: 82.886 Y: 69.162 Z: 85.346
	6.99 / (2)	X: 80.526 Y: 73.635 Z: 76.563
	4.07 / (3)	X: 76.070 Y: 74.062 Z: 91.088
	2.68 / (4)	X: 88.075 Y: 76.004 Z: 85.065
	2.40 / (5)	X: 83.025 Y: 55.252 Z: 86.628
Modbase Best	16.37 / (1)	X: 7.927 Y: 9.358 Z:17.850
	7.07/ (2)	X: 10.183 Y: 12.963 Z: 25.547
	3.04/ (3)	X: 35.079 Y: 6.699 Z: 24.505

	1.87/ (4)	X: 6.036 Y: 4.553 Z: 28.994
	1.63 / (5)	X: 8.005 Y: -4.611 Z: -8.027
Phyre Best	8.47 / (1)	X: 48.045 Y: 58.722 Z: -18.113
	8.02 / (2)	X: 38.443 Y: 56.890 Z: -24.320
	6.14 / (3)	X: 37.105 Y: 74.690 Z: -40.169
	4.63 / (4)	X: 53.472 Y: 55.475 Z: -9.904
	3.62 / (5)	X: 33.303 Y: 69.549 Z: -20.714
Schrödinger AA best	8.94 / (1)	X: 54.319 Y: 57.018 Z: -9.344
	8.37 /(2)	X: 38.310 Y: 57.088 Z: -24.309
	6.96 /(3)	X: 38.340 Y: 74.779 Z: -39.934
	6.71 / (4)	X: 46.371 Y: 57.152 Z: -17.869
	2.25 / (5)	X: 56.951 Y: 67.605 Z: -43.553

Based on the data produced, we will use the top 3 binding sites from each protein structure to perform the docking calculations of the hit compound and locate the most probable binding site.

2.2.2. Specific Aim 2: Molecular docking of hit compound and novel determination of drugs for EAAT3 protein model

With the identification of the binding sites we now proceed to dock lidocaine to find where is the best fit among the different binding sites among the different protein models. We have selected lidocaine (figure 5) as our hit compound because it is one of the molecules that activate the EAAT3 transporter; additionally, lidocaine has a well-established synthetic path. Lidocaine is a well-known voltage-gated sodium channel blocker and it works in the cell membrane of post-synaptic neurons, preventing depolarization and inhibiting the generation and propagation of nerve impulses.[81] Even though this molecule has been extensively studied, the molecular binding mechanism has not been completely elucidated. Lidocaine is widely used as a local anesthetic, but it can also be used to treat ventricular arrhythmias and acute coronary syndrome associated with the toxicity of various stimulants.[5,79] The drug is able to cross the blood brain barrier and can be administered topically (drug penetrates the skin and reaches the nerves to produce analgesia without numbness), orally, inhaled, or injected.[5,79] In terms of pharmacokinetics, the average half-life of lidocaine in adults is 1.5–2 hours; however, it may be prolonged in patients receiving lidocaine infusions for periods longer than 24 hours.[79] Finally, lidocaine is metabolized in the liver by de-ethylation to form monoethylglycinexylidide and glycine xylidide, followed by cleavage of the amide bond to form xylidine and 4-hydroxyxylidine,

which are excreted in urine. It is possible that lidocaine is binding to an important motif that locks the EAAT3 protein in a certain conformation, allowing it to transport more glutamate.

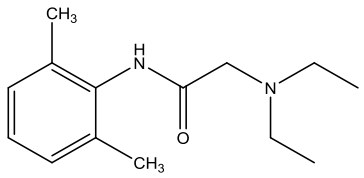

Figure 5. Illustration of Lidocaine

The docking calculations were done with Vina AutoDock4. AutoDock4, is an empirical scoring function that approximates the ligand binding free energy. This docking function is based on electrostatic, Van der Waals and other functions, i.e. column energy, and internal ligand strain, among other parameters.[60] The scoring function is provided in figure 6. The docking parameters that we employed were the Lamarckian genetic algorithm with 2,500,000 evaluations. As for ligand parameters, we allowed all of the possible torsion the ligand could have. We decided to use the Lamarckian genetic algorithm because is a reliable and efficient method to predict the docking conformation of protein ligand complexes.

$$\Delta G = (V_{bound}^{L-L} - V_{unbound}^{L-L}) + (V_{bound}^{P-P} - V_{unbound}^{P-P}) + (V_{bound}^{P-L} - V_{unbound}^{P-L} + \Delta S_{conf})$$

$$V = W_{vdw}\sum_{i,j}\left(\frac{A_{ij}}{r_{ij}^{12}} - \frac{B_{ij}}{r_{ij}^{6}}\right) + W_{hbond}\sum_{i,j}E(t)\left(\frac{C_{ij}}{r_{ij}^{12}} - \frac{D_{ij}}{r_{ij}^{10}}\right) + W_{elec}\sum_{i,j}\frac{q_i q_j}{e(r_{ij})r_{ij}} + W_{sol}\sum_{i,j}\left(S_i V_j + S_j V_i\right)e^{(-r_{ij}^2/2\sigma^2)}$$

Figure 6. Gibbs free energy is calculated by six pair-wise evaluations (V) and an estimate of the conformational entropy lost upon binding. The energetic terms includes evaluations for dispersion/repulsion, hydrogen bonding, electrostatics, and desolvation.[60]

After docking lidocaine to the different binding sites in the different protein models, we evaluated the protein ligand interactions. Data for the dockings of lidocaine with the target proteins in the different binding pockets is given in table 10. Overall, if we take a close look at the amino acids and the locations of the binding pocket of each protein, we can observe that the binding pockets are not so far apart from one another. Figure 7 contains an illustration of the protein with the best docking results accompanied by the amino acids interacting with the molecule.

Table10. Molecular docking results from the molecular dockings of lidocaine with the top 3 elucidated binding pockets.

Protein model	Binding pocket 1	Binding pocket 2	Binding pocket 3
ITASSER best	Coordinates of binding pocket: X:82.89;Y:69.16;Z:85.35 Binding_energy=-5.87 Ligand_Efficiency=-0.35 Inhib_constant=50.17uM AA involved in H-Bond: ASN 241	Coordinates of binding pocket: 80.53 73.64 76.56 Binding energy=-5.88 Ligand Efficiency=-0.35 Inhib constant=49.1uM AA involved in H-Bond: ASN 241	Coordinates of binding pocket: 76.07 74.06 91.09 Binding energy=-6.34 Ligand Efficiency=-0.37 Inhib constant=22.55uM AA involved in H-Bond: GLN 252
Modbase best	Coordinates of binding pocket: X:17.85; Y:7.93; Z: 9.36	Coordinates of binding pocket:	Coordinates of binding pocket: X:35.08; Y:6.70; Z:24.51

	Binding_energy=-6.49 Ligand_Efficiency=-0.38 Inhib_constant=17.56uM AA involved in H-Bond: Thr364 and THR 185	X:25.55; Y:10.18; Z:12.96 Binding_energy=-6.67 Ligand_Efficiency=-0.39 Inhib_constant=12.84uM AA involved in H-Bond: Thr364 and THR 185	Binding_energy=-5.82 Ligand_Efficiency=-0.34 Inhib_constant=54.23uM AA involved in H-Bond: ASN 195
Phyre best	Coordinates of binding pocket: X:48.05; Y:58.72; Z:-18.11 Binding_energy=-6.21 Ligand_Efficiency=-0.37 Inhib_constant=28.2uM AA involved in H-Bond: ARG 447	Coordinates of binding pocket: X:38.44; Y:56.89; Z:-24.32 Binding_energy=-5.57 Ligand_Efficiency=-0.33 Inhib_constant=82.51uM AA involved in H-Bond: LEU 68	Coordinates of binding pocket: X:37.11; Y:74.69; Z:-40.17 Binding_energy=-5.44 Ligand_Efficiency=-0.32 Inhib_constant=102.86uM AA involved in H-Bond: VAL 20
Schrödinger best	Coordinates of binding pocket: X:54.32; Y:57.02; Z:-9.34	Coordinates of binding pocket: X:38.31; Y:57.09; Z:-24.31	Coordinates of binding pocket: X:38.34; Y:74.78; Z:-39.93

	Binding_energy=-5.45 Ligand_Efficiency=-0.32 Inhib_constant=101.11 uM AA involved in H-Bond: None	Binding_energy=-5.53 Ligand_Efficiency=-0.33 Inhib_constant=88.66u M AA involved in H-Bond: LEU 68	Binding_energy=-5.87 Ligand_Efficiency=-0.35 Inhib_constant=50.06uM AA involved in H-Bond: VAL 20

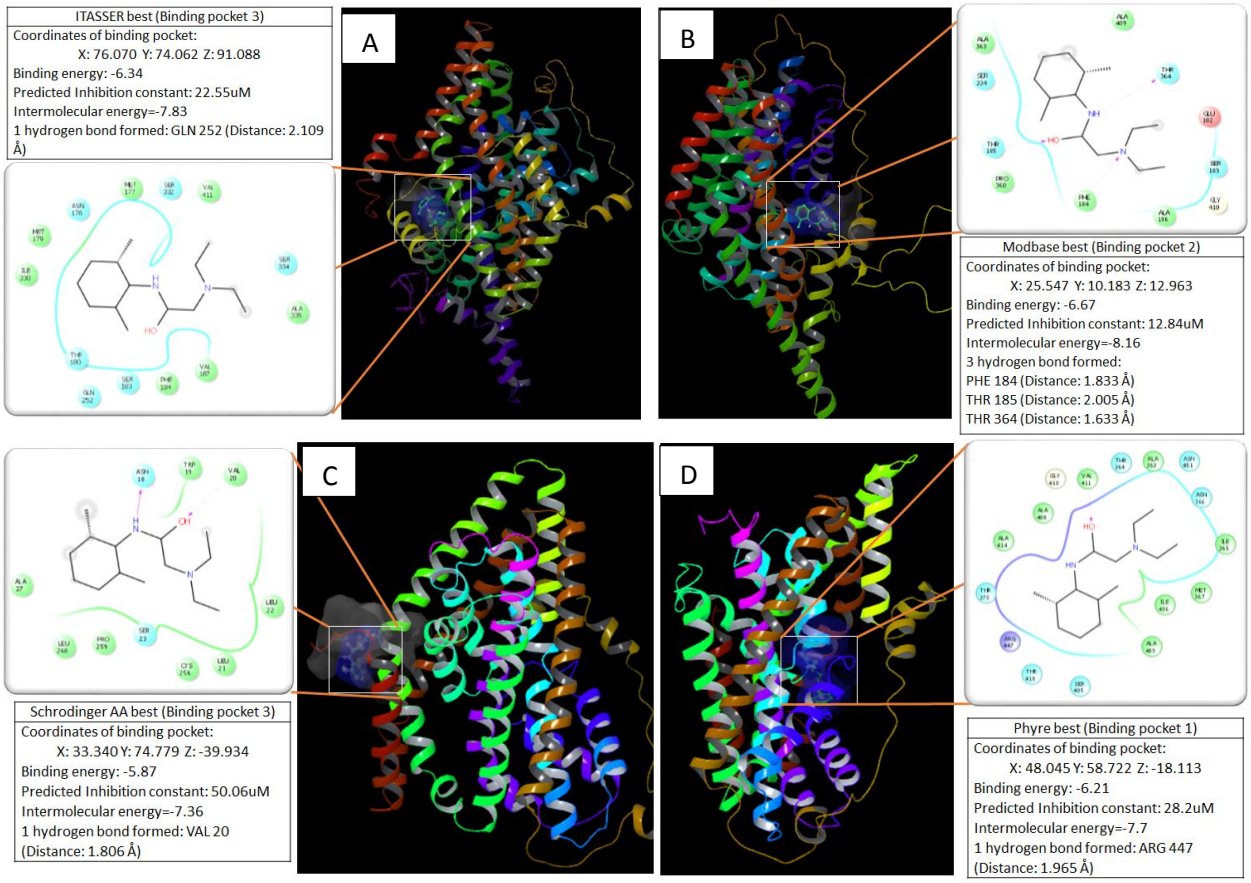

Figure 7. Best protein models binding pockets and amino acid interactions with lidocaine A) ITASSER model best B) Modbase best C) Schrödinger AA best D) Phyre best. Each illustration contains a small description of the binding pocket coordinates, binding scores, and H-bonding interactions.

Based on the docking scores of lidocaine, we decided to create new lidocaine analogs to develop a more stable protein-ligand binding complex. Additionally, we screened (docked) molecular fragments to identify new compounds that will bind more efficiently to EAAT3. The lidocaine analogs were tailored to evaluate the binding patterns and structural scaffolds of non-covalent interactions (Van der Waals, electrostatic, H-Bond, Halogen bond, and hydrophobic bonding) in the binding pocket. Table 11 explains more in detail the purpose of each modification and, additionally, it gives a potential synthetic scheme by which these molecules can be made. The theory of halogen bonding states that when halogen (usually Cl, Br or I) is bonded to a strong electron-withdrawing group, its valence shell electrons will be polarized toward the side of the electron-withdrawing group, creating a partial positive charge in the Pz electron orbital, allowing the halogen to act as Lewis acid; this phenomenon is known as polar flattening.[59,61] The major advantage of halogen bonding is that it does not interfere with hydrogen bonding; however, this is a very directional interaction.[62,63]

Table 11. Designed Docking analogs and their respective synthetic routes for further elucidation of binding parameters of EAAT3.

Lidocaine Analog	Rationale	Structure
LA1	We will substitute the diethyl amine motif of lidocaine for vanillin. The purpose of this analog is to increase the hydrophobicity, and increase the hydrogen bond network through the structure.	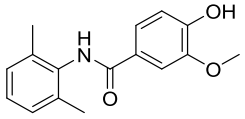

<table>
<tr><td colspan="3"> 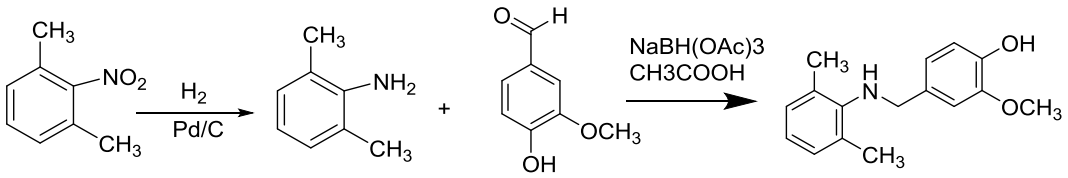 </td></tr>
<tr><td>LA2</td><td>We will substitute the diethyl amine motif of lidocaine for an aromatic complex. The objective is to increase the hydrophobicity and aromaticity of the molecule, producing a more feasible binding to an important hydrophobic pocket.</td><td> 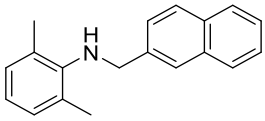 </td></tr>
<tr><td colspan="3"> 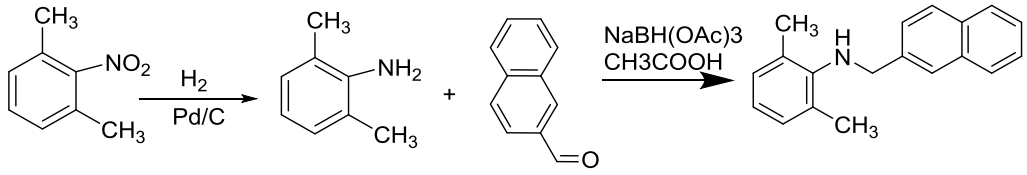 </td></tr>
<tr><td>LA3</td><td>We will substitute 2,6-dimethylnitrobenzene with naphthalene to increase hydrophobicity at the other end of the molecule, in comparison with the LA2 analog.</td><td> 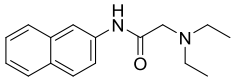 </td></tr>
<tr><td colspan="3"> 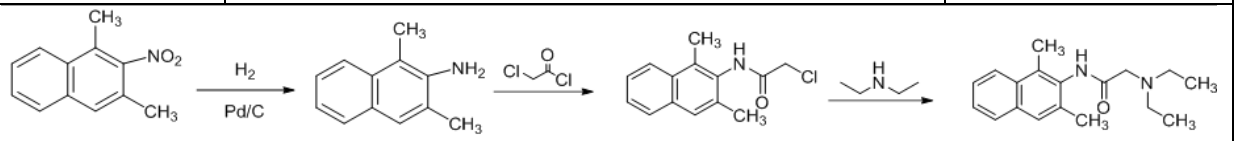 </td></tr>
<tr><td>LA4</td><td>We will increase the bulkiness of the compound without the π-π electron cloud of a conjugated aromatic ring, like in the LA3 analog.</td><td> 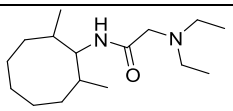 </td></tr>
</table>

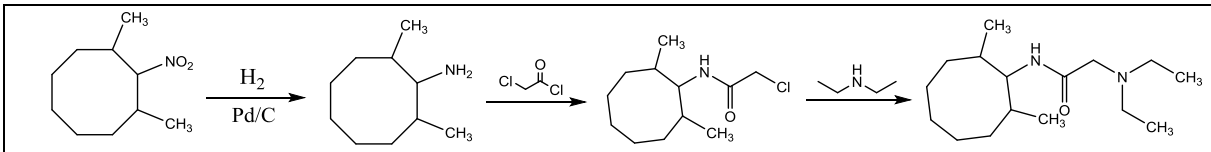

LA5	We will increase the length of the molecule by adding more saturated hydrocarbons, thus increasing the surface area on which the protein interacts with the molecule.	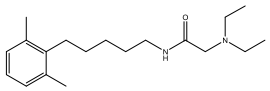

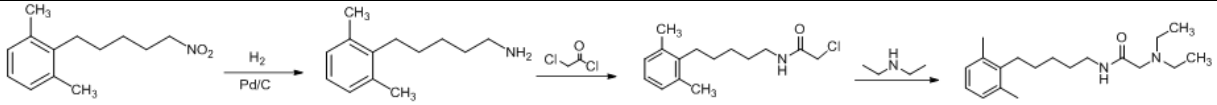

LA6	We will add a bromine in the 2,6-dimethylnitrobenzene, in an attempt to use the unique properties of the **σ**-hole produced by the halogenated compounds.	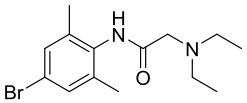

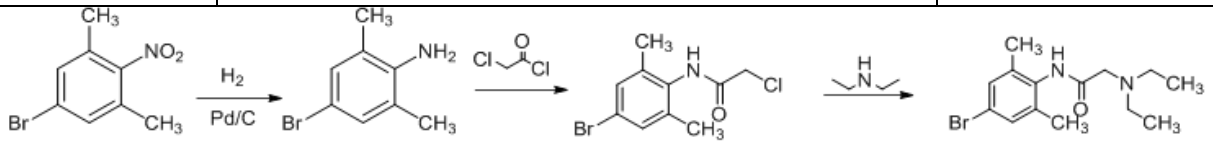

Before beginning the binding of the lidocaine analogs, it was important to obtain a correct molecular geometry because docking scores can be greatly affected by the structural orientation of chemical bonds. With this in mind, we optimized the molecular geometry of the proposed analogs to obtain a reliable molecular structure. For this optimization we used a density functional theory calculation with a b3lyp/6-31g basis set.[64] The optimized molecules were then

docked to the different protein models in the location where lidocaine had the highest docking scores. The majority of the analogs increased the docking scores; however, the highest docking scores correspond to the lidocaine anlalog 2 (LA2). The mayor advantage of this analog is the aromatic rings that give a more planar structure to the molecule, and also increase the hydrophobic surface area. LA3 is structurally similar to LA2 and their docking scores are close to one another, and even though the ketone and the diethyl amine motif establish hydrogen bonds to the binding pocket, they were not enough to surpass the hydrophobic interactions brought by LA2. The analogs LA4 and LA5 also increase the hydrophobic surface area, but their docking scores are the lowest among the analogs; this could be because the structures are more flexible than in LA2, not allowing it to make contact and establish all the possible interactions available between the alpha helixes. LA1 has an extended hydrogen bond network and it manages to create several hydrogen bonds in the binding pocket; however, the binding pocket seemed to be dominated by hydrophobic interactions. In the case of LA6 the halogen bond did not bring any significant advantages to their particular binding site; this could be due to the fact that halogen bonds are very directional and they require very strong electron-withdrawing groups to make use of their interactions. From this analysis we can infer that the interactions in the binding pocket are dominated by hydrophobic interactions, and that contributions from a planar conjugated aromatic system are better able to accommodate the binding pocket.

We obtained information about the ADMET[10] (absorption, distribution, metabolism, excretion, and toxicity) of lidocaine and the analogs. The AMED scores for lidocaine and the analogs are provided in the appendix section E.3. All of the ADMET calculations were done using the web servers AMEDstar, ACD/I and Schrödinger Maestro (AMED). Once we completed the

docking and molecular dynamic studies, we determined the best molecules based on their binding energy and ADMET scores. This process allowed us to select a molecule that will have low toxicity, high binding efficiency, and higher probability of being absorbed by the body. Within the ADMET calculations, the Lipinski's rules help in calculating the fate of a drug that is going to be orally administered. The Lipinski's rules are a set of rules which, if followed, might give a molecule a higher probability to be absorbed and to permeate the cell membrane. These rules are based on the physico-chemical properties of a molecule. The Lipinski's rules are the following, with no particular order: the molecular weight of the protein must not exceed 500 g/mol, the $LogP_{ow}$ (water/octanol partition coefficient) must be less than 5, and the number of hydrogen bond donors/acceptors muss be less than 5/10 respectively.[65] Additionally, a polar surface area less than 90 angstroms squared is usually needed. The Lipinsky's rules should not be taken as a gold standard, but rather a set of guidelines that might increase a molecule's oral bioavailability.[66] We have also taken into consideration the hERG score, a parameter based on the blockade of the hERG potassium channel, which presents a significant risk of arrhythmia (QT prolongation) in clinical application. The hERG score calculates the affinity of a particular molecule to bind to this particular channel. If the hERG score is high, it represents a potential risk to the patient.[67,68]

Our next goal was to create a new library of compounds to bind to the EAAT3 protein. For this we used a program called Open Growth v0.430.[71] This programs constructs *de novo* ligands by placing small organic fragments into the binding pocket. The first fragment is rotated at random orientations in the binding pocket until the lowest score is achieved. After the first fragment is placed, the second fragment is inputted, and once the search is complete for the

second fragment, the program attempts to bind these 2 fragments. The search continues until N number of fragments are inputted. In this particular study, we selected the top 10 constructed ligands derived from the organic fragments that received the lowest scores from the data. The program uses a knowledge-based potential to calculate binding affinities (SMOG2015). To start the calculation, we defined the binding site of the protein models, which was the same binding site we used to dock the lidocaine analogs. We set the parameters to construct a maximum of 200 ligands per protein model, and the library that we used to construct those ligands is the default fragment library of 113 fragments provided by the Open Growth program. Once the program constructs a ligand, it is going to optimize its geometry and position to better accommodate the binding pocket. In this study, the force field used to optimize the molecules is the MMFF94 force field; each ligand is going to be optimized 30 times with 10 iterations each time it changes its position or moves its dihedral angle. Finally, the last parameters inputted into the program were that the molecule must not surpass the 600 g/mol in molecular weight, and when the growth process reached 200 ligands, it would stop the construction of ligand molecules. The results from this program yielded 200 new ligands per protein binding pocket; since we are using the four best protein models, we obtained 800 new ligands in total. The top ten ligands per protein model are given in the figures below (Figure 8- Figure 11). The ligands are arranged by their docking scores, the more negative the docking score, the more likely they are to successfully bind to the designated binding pocket.

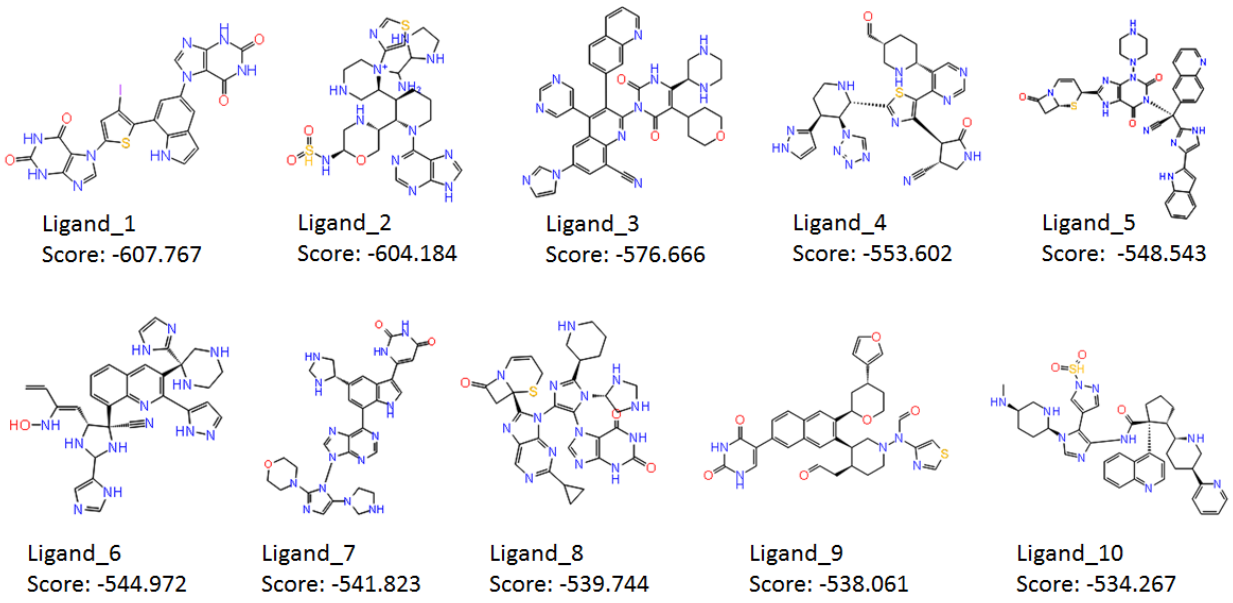

Figure 8. Top ten de novo ligands created from small organic fragment molecules for the Modbase best protein model and binding pocket.

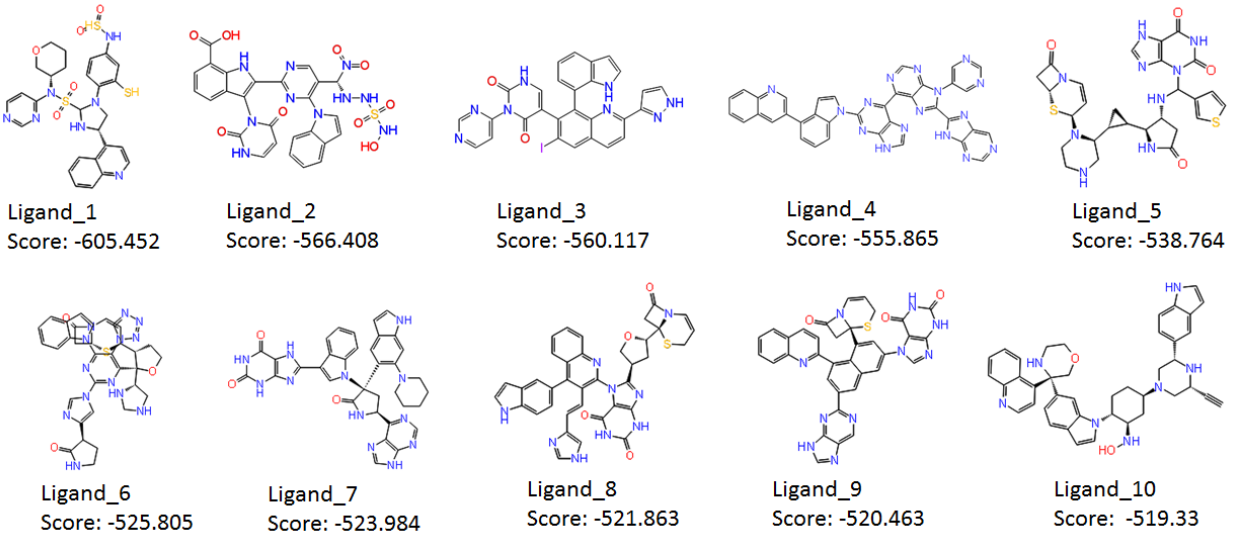

Figure 9. Top ten de novo ligands created from small organic fragment molecules for the ITASSER best protein model and binding pocket.

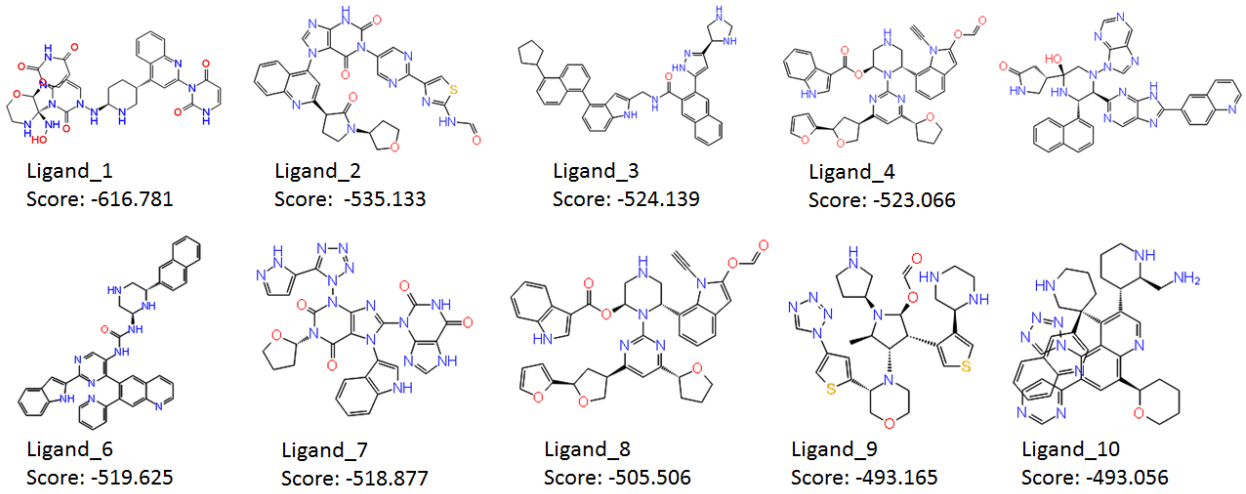

Figure 10. Top ten de novo ligands created from small organic fragment molecules for the Phyre best protein model and binding pocket.

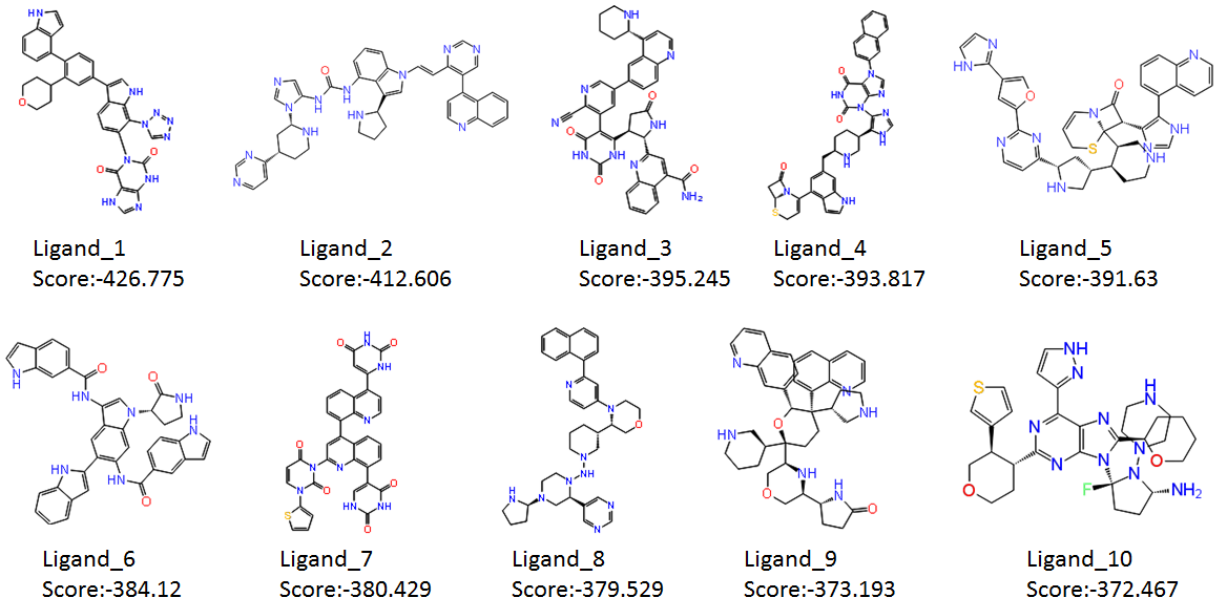

Figure 11. Top ten de novo ligands created from small organic fragment molecules for the Schrödinger best protein model and binding pocket.

Overall, we can observe that most of the new constructed ligands have similar characteristics. Most of the ligands have aromatic rings; the most prominent feature among the aromatic structures is the naphthalene ring fragment, which is particularly useful to increase the hydrophobicity of the molecule. We saw the same trend when we created and docked the

lidocaine analogs: having a naphthalene motif was very beneficial when compared to the other modifications; however, then main disadvantage of introducing aromatic groups is that they tend to increase the toxicity of the molecules. We can also observe that most molecules have pyrimidine, pyridine, ketones, and tetrahydropyran fragments associated with their structure. These particular motifs allow the molecule to extend its hydrogen bond network. Additionally, we can also observe some fragments making use of halogens; this can be due to their halogen-bonding capabilities, or simply because halogens are very electronegative groups that withdraw electron density from allowing the atom or group that is bonded to become more electropositive, thus allowing the possibility of electrostatic interactions to occur. The main drawback of this study is that even though we might have created molecules that are going to have a superior binding affinity to the target molecule, developing a synthetic scheme for these molecules can be a cumbersome task. Overall we can observe that the top molecules all have common characteristics. Even though the study was conducted in different protein models, with each protein model having its own binding pocket, this is a good agreement in the qualities a good ligand should have for it to be successful in obtaining a high binding affinity in the magnitude on nanomoles.

2.2.3. Specific Aim 3: Molecular dynamic calculations of the best protein – ligand models

To make our results emulate the physiological conditions, and to further analyze the docking interaction between the protein and the ligand, we performed molecular dynamics on the docked ligands. We first placed the protein in a solvated state, neutralized the protein charges with Na^+ or Cl^- ions, and surrounded it in a 1-palmitoyl-2-oleoyl-snglycero-3-phosphocholine (POPC) phospholipid bilayer. The reason to use a lipid layer is because EAAT3 is

a membrane protein, so in physiological conditions, which we are trying to emulate, the proteins would be embedded in a lipid membrane. Besides the lipid membrane, we also used the NPγT ensemble class at a temperature of 300K, pressure 1.01325 bar, and surface tension of 4000.0 bar•Å. The molecular dynamics calculation was done using the Desmond Molecular Dynamics package, and we used the standard desmond force field parameters (figure 12). We ran the molecular dynamics simulation for .12 nanoseconds with recording intervals of 1.2 picosecounds to evaluate the stability of the ligand and to observe any relevant changes in conformation. With this information, we were able to observe which molecule forms a more stable complex.

$$U = U_{\text{bonded}} + \sum_{(i,j)\in N} U_{\text{vdW}} + \sum_{(i,j)\in N} q_i q_j \text{erfc}(r_{ij}/\sqrt{2}\sigma)/r_{ij} + \sum_{(i,j)\in N} q_i q_j \text{erf}(r_{ij}/\sqrt{2}\sigma)/r_{ij} - \sum_{(i,j)\notin N} q_i q_j \text{erf}(r_{ij}/\sqrt{2}\sigma)/r_{ij}$$

Figure 12. Mathematical representation of the DESMOND Force field.[20]

We only ran the molecular dynamics for the protein–ligand interaction of the best EAAT3 models docked with lidocaine, our hit compound. We used the Root Mean Square Deviation (RMSD) to measure the change in position of a selection of atoms for a particular frame with respect to a reference frame. Figures 13-16 present the results from the molecular dynamics calculations of the best protein models docked with lidocaine. We can observe in panel B) from all of the protein models that they don't make significant local changes along the protein chain.

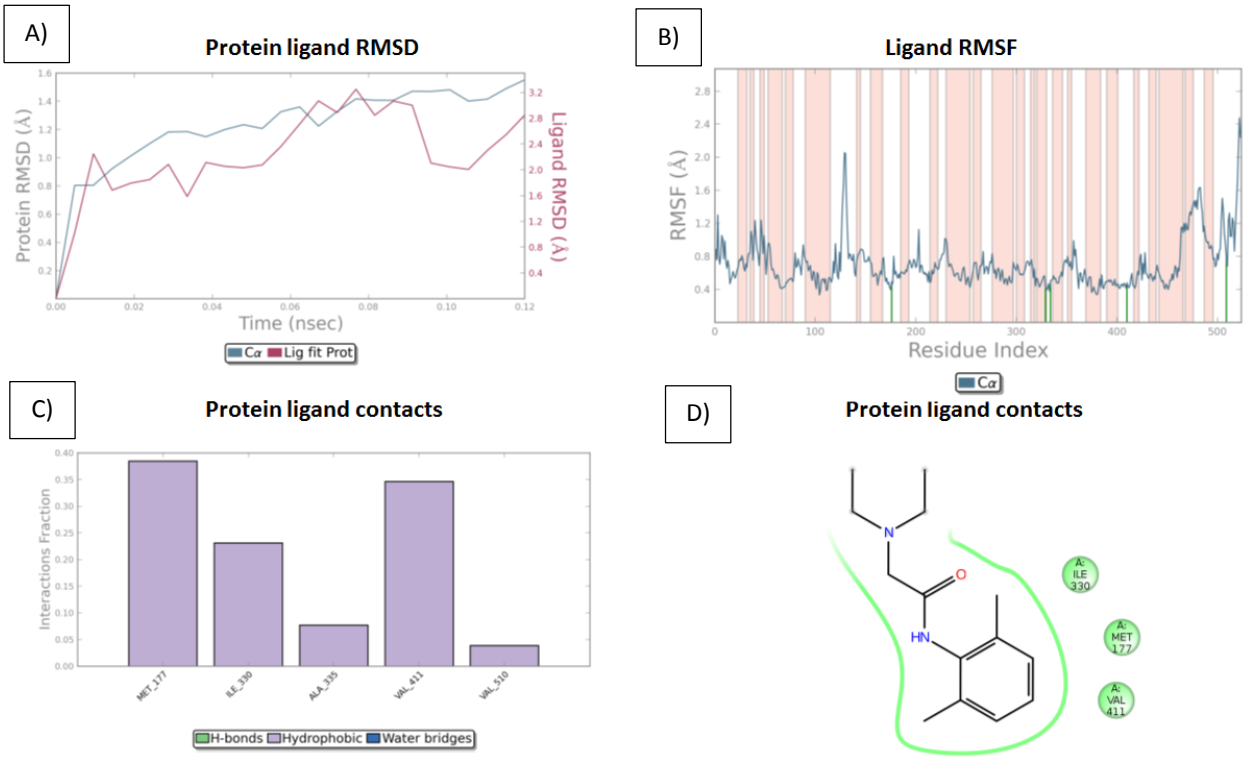

Figure 13. ITASSER results for the molecular dynamic studies. A) Measure the displacement of protein ligand complex in RMSD units as a function of time in nanoseconds. B) The pink highlighted sections of the graph represent the secondary structure of the protein. Ligand interactions are marked in green. C) Gives a normalized graphical representation of the protein ligand contacts to observe and identify the mayor contributor in binding. D) Graphical representation of the mayor interactions in the binding pocket with lidocaine.

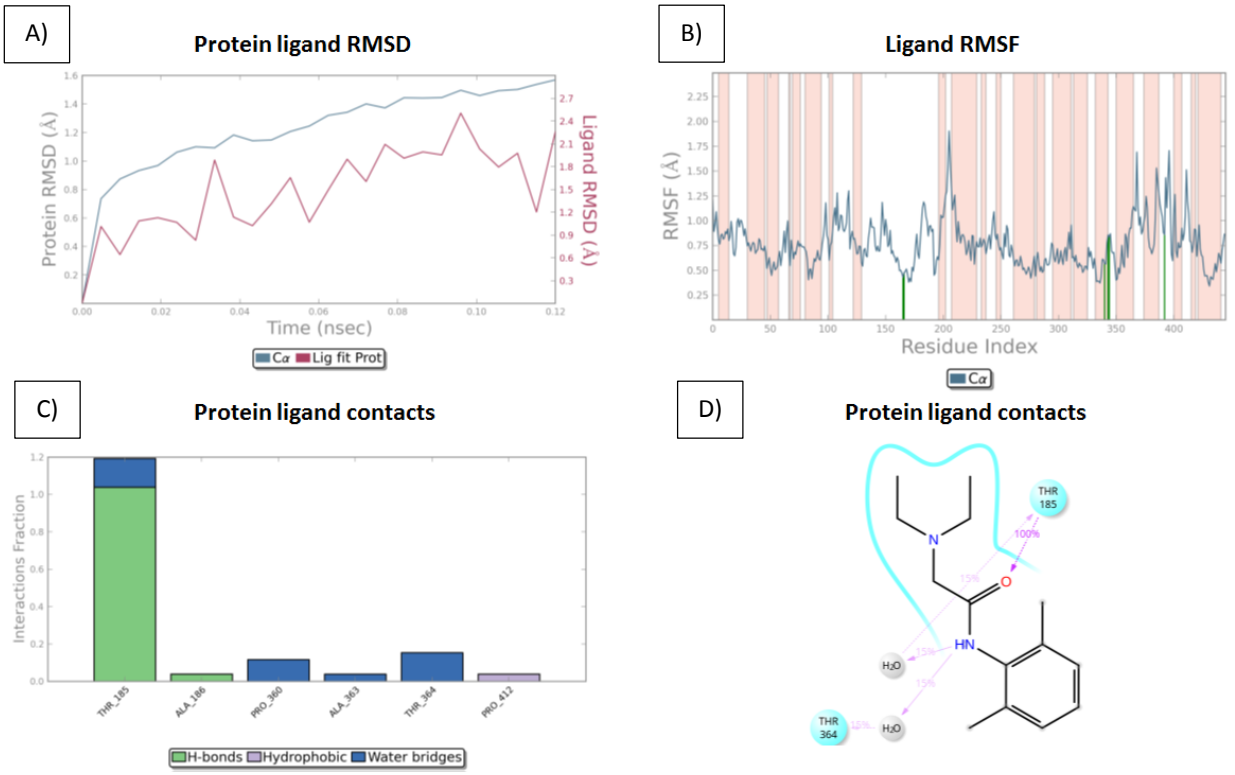

Figure 14. Modbase results for the molecular dynamic studies. A) Measure the displacement of protein ligand complex in RMSD units as a function of time in nanoseconds. B) The pink highlighted sections of the graph represent the secondary structure of the protein. Ligand interactions are marked in green. C) Gives a normalized bar graph representation of the protein ligand contacts to observe and identify the mayor contributor in binding. D) Graphical representation of the mayor interactions in the binding pocket with lidocaine.

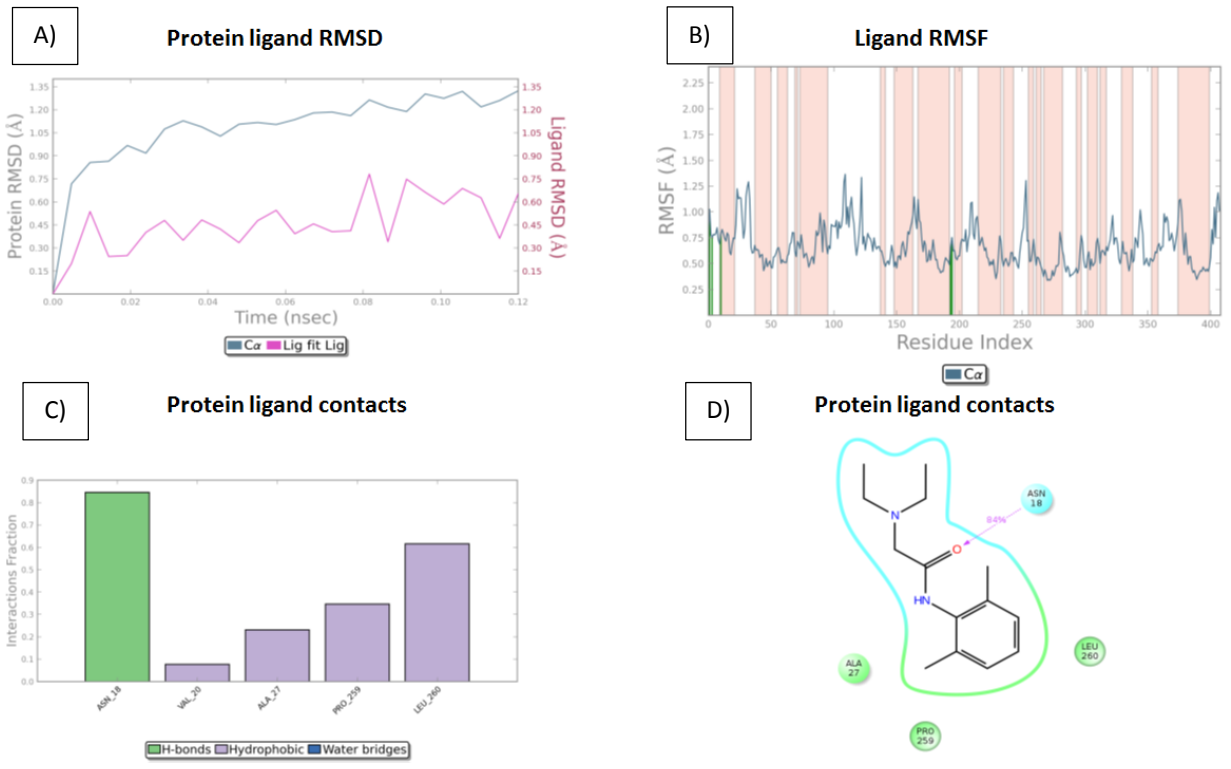

Figure 15. Phyre results for the molecular dynamic studies. A) Measure the displacement of protein ligand complex in RMSD units as a function of time in nanoseconds. B) The pink highlighted sections of the graph represent the secondary structure of the protein. Ligand interactions are marked in green. C) Gives a normalized graphical representation of the protein ligand contacts to observe and identify the mayor contributor in binding. D) Graphical representation of the mayor interactions in the binding pocket with lidocaine.

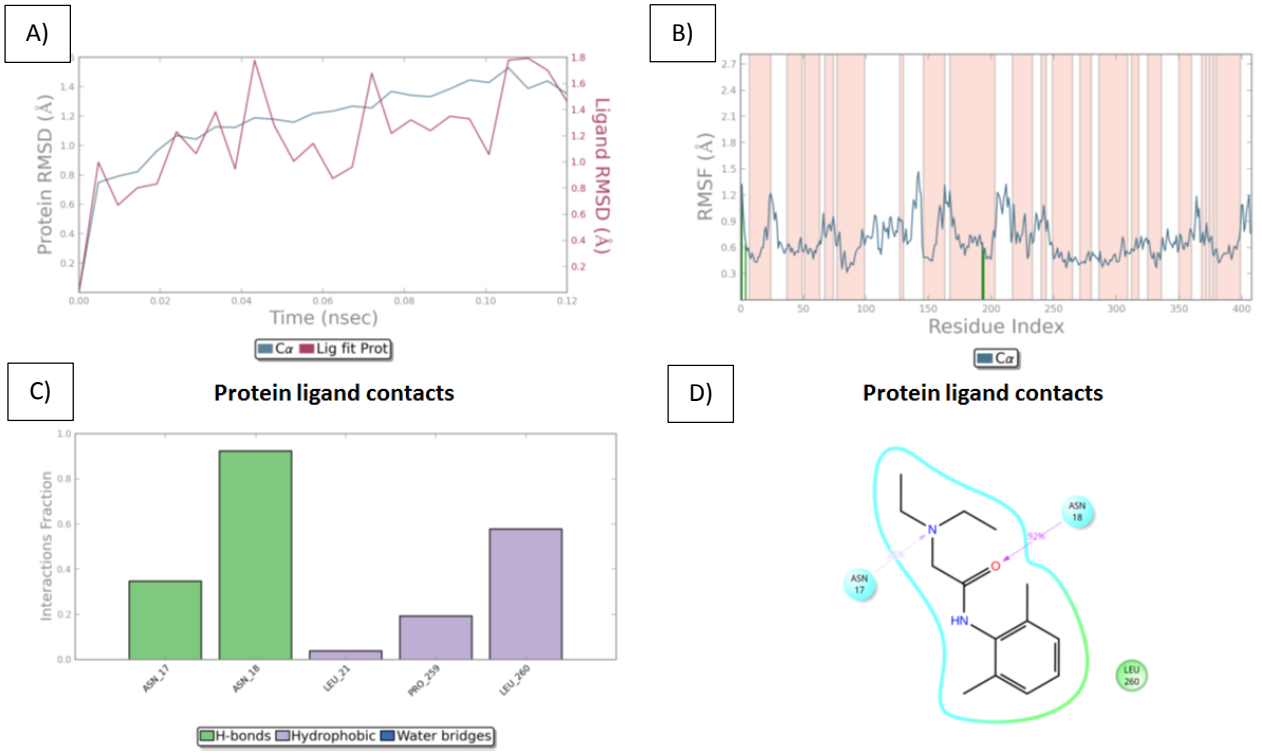

Figure 16. Schrodinger results for the molecular dynamic studies. A) Measure the displacement of protein ligand complex in RMSD units as a function of time in nanoseconds. B) The pink highlighted sections of the graph represent the secondary structure of the protein. Ligand interactions are marked in green. C) Gives a normalized graphical representation of the protein ligand contacts to observe and identify the mayor contributor in binding. D) Graphical representation of the mayor interactions in the binding pocket with lidocaine.

From this study we can conclude that, even though we have different protein models and each model has its own binding pocket, we find very similar characteristics in regard to overall structure, ligand scores, ligand construction patterns, and molecular dynamic calculations. The elucidated binding pockets among the different protein models make use of hydrophobic interactions to dock the ligand, and when lidocaine is modified to have more hydrophobic groups, the docking scores increase in all protein models in all binding pockets. We can also observe this pattern in the protein ligand contacts, which reveal that most of the interactions are hydrophobic in nature. There might be hydrogen bonding as in the case of ITASSER and Phyre models; however, the sum of the hydrophobic interactions surpasses the contribution of the hydrogen bonds. Molecular dynamics also reveal that there is little conformational changes in the

protein ligand binding pocket; however, to make this study more comprehensive, a longer molecular dynamic calculation is needed. It is suggested to run a 10 to 15 ns molecular dynamics calculation.

REFERENCES

[1] Center for Addiction and Mental Health. (2012). "Treatments for OCD: Medications." Retrieved 3 February, 2015, from http://www.camh.ca/en/hospital/health_information/a_z_mental_health_and_addiction_information/obsessive_compulsive_disorder/obsessive_compulsive_disorder_information_guide/Pages/ocd_medications.aspx.

[2] Charles G., W., Reed, M., "Natural Healing of Obsessive Compulsive Disorder (OCD)." International guide to the world of alternative mental health. Retrieved 3 February 2015, from http://www.alternativementalhealth.com/articles/ocd.htm.

[3] Mayo Clinic. (2013). "Obsessive-compulsive Disorder (OCD)." Diseases and Conditions. Retrieved 3 February 2015 from http://www.mayoclinic.org/diseases-conditions/ocd/basics/definition/con-20027827.

[4] Bokor, G. and P. D. Anderson (2014). "Obsessive-compulsive disorder." J Pharm Pract 27(2): 116-130.

[5] Markarian, Y., et al. (2010). "Multiple pathways to functional impairment in obsessive-compulsive disorder." Clin Psychol Rev 30(1): 78-88.

[6] Mushtaq A. M., et al. (2014) "Treatment-Resistant Obsessive-Compulsive Disorder (OCD) – Current Understanding." InTech, DOI: 10.5772/57232. Retrieved 3 February 2015 from: http://www.intechopen.com/books/obsessive-compulsive-disorder-the-old-and-the-new-problems/treatment-resistant-obsessive-compulsive-disorder-ocd-current-understanding.

[7] Albelda, N. and D. Joel (2012). "Animal models of obsessive-compulsive disorder: exploring pharmacology and neural substrates." Neurosci Biobehav Rev 36(1): 47-63.

[8] Campiani, G., et al. (2001). "A rational approach to the design of selective substrates and potent nontransportable inhibitors of the excitatory amino acid transporter EAAC1 (EAAT3). new glutamate and aspartate analogues as potential neuroprotective agents." J Med Chem 44(16): 2507-2510.

[9] Case D.A., Babin V., Berryman J.T., Betz R.M., Cai Q., Cerutti D.S., T.E. Cheatham, III, T.A. Darden, R.E. Duke, H. Gohlke, A.W. Goetz, S. Gusarov, N. Homeyer, P. Janowski, J. Kaus, I. Kolossváry, A. Kovalenko, T.S. Lee, S. LeGrand, T. Luchko, R. Luo, B. Madej, K.M. Merz, F. Paesani, D.R. Roe, A. Roitberg, C. Sagui, R. Salomon-Ferrer, G. Seabra, C.L. Simmerling, W. Smith, J. Swails, R.C. Walker, J. Wang, R.M. Wolf, X. Wu and P.A. Kollman (2014), AMBER 14, University of California, San Francisco. http://ambermd.org/contributors.

[10] Eddershaw, P. J., et al. (2000). "ADME/PK as part of a rational approach to drug discovery." Drug Discov Today 5(9): 409-414.

[11] Heinzelmann, G. and S. Kuyucak (2014). "Molecular dynamics simulations elucidate the mechanism of proton transport in the glutamate transporter EAAT3." Biophys J 106(12): 2675-2683.

[12] Robinson, L. J. and M. H. Freeston (2014). "Emotion and internal experience in Obsessive Compulsive Disorder: reviewing the role of alexithymia, anxiety sensitivity and distress tolerance." Clin Psychol Rev 34(3): 256-271.

[13] Nathan, P. J., et al. (2006). "The neuropharmacology of L-theanine(N-ethyl-L-glutamine): a possible neuroprotective and cognitive enhancing agent." J Herb Pharmacother 6(2): 21-30.

[14] Heinzelmann, G. and S. Kuyucak (2014). "Molecular dynamics simulations of the mammalian glutamate transporter EAAT3." PLoS One 9(3): e92089.

[15] O'Kane, R. L., et al. (1999). "Na(+)-dependent glutamate transporters (EAAT1, EAAT2, and EAAT3) of the blood-brain barrier. A mechanism for glutamate removal." J Biol Chem 274(45): 31891-31895.

[16] Brennan, B. P., et al. (2013). "A critical review of magnetic resonance spectroscopy studies of obsessive-compulsive disorder." Biol Psychiatry 73(1): 24-31.

[17] Wu, K., et al. (2012). "The role of glutamate signaling in the pathogenesis and treatment of obsessive-compulsive disorder." Pharmacol Biochem Behav 100(4): 726-735.

[18] Kariuki-Nyuthe, C., et al. (2014). "Obsessive compulsive disorder and the glutamatergic system." Curr Opin Psychiatry 27(1): 32-37.

[19] Arnold K., Bordoli L., Kopp J., and Schwede T. (2006). The SWISS-MODEL Workspace: A web-based environment for protein structure homology modelling. Bioinformatics, 22,195-201.

[20] Niciu, M. J., et al. (2012). "Overview of glutamatergic neurotransmission in the nervous system." Pharmacol Biochem Behav 100(4): 656-664.

[21] Sarris, J., et al. (2012). "Complementary medicine, self-help, and lifestyle interventions for obsessive compulsive disorder (OCD) and the OCD spectrum: a systematic review." J Affect Disord 138(3): 213-221.

[22] Pauls, D. L., et al. (2014). "Obsessive-compulsive disorder: an integrative genetic and neurobiological perspective." Nat Rev Neurosci 15(6): 410-424.

[23] Mattheisen, M., et al. (2014). "Genome-wide association study in obsessive-compulsive disorder: results from the OCGAS." Mol Psychiatry.

[24] Taylor, S. (2013). "Molecular genetics of obsessive-compulsive disorder: a comprehensive meta-analysis of genetic association studies." Mol Psychiatry 18(7): 799-805.

[25] Wang, L., et al. (2009). "Assessing the validity of current mouse genetic models of obsessive-compulsive disorder." Behav Pharmacol 20(2): 119-133.

[26] Jenike, M. and Dailey, S. “Sudden and Severe Onset OCD (PANS/PANDAS) – Practical Advice for Practitioners and Parents” International OCD Foundation Retrieved. 3 February 2015, from http://iocdf.org/pandas/.

[27] National Institute of Mental Health (NIMH)." PANDAS: Frequently Asked Questions about Pediatric Autoimmune Neuropsychiatric Disorders Associated with Streptococcal Infections." National Institute of Health. Retrieved. 3 February 2015, from http://www.nimh.nih.gov/health/publications/pandas/index.shtml

[28] Guex, N., Peitsch, M.C., Schwede, T. (2009). Automated comparative protein structure modeling with SWISS-MODEL and Swiss-PdbViewer: A historical perspective. Electrophoresis, 30(S1), S162-S173.

[29] Do, S. H., et al. (2002). "The effects of lidocaine on the activity of glutamate transporter EAAT3: the role of protein kinase C and phosphatidylinositol 3-kinase." Anesth Analg 95(5): 1263-1268, table of contents.

[30] Do, S. H., et al. (2002). "Effects of volatile anesthetics on glutamate transporter, excitatory amino acid transporter type 3: the role of protein kinase C." Anesthesiology 96(6): 1492-1497.

[31] Burguiere, E., et al. (2013). "Optogenetic stimulation of lateral orbitofronto-striatal pathway suppresses compulsive behaviors." Science 340(6137): 1243-1246.

[32] Jonsson, H., et al. (2011). "Randomized comparative study of group versus individual cognitive behavioural therapy for obsessive compulsive disorder." Acta Psychiatr Scand 123(5): 387-397.

[33] Wayne K., Goodman, M. (2013, 30 Jan. 2013). "Treatments for Obsessive-compulsive Disorder." Retrieved 3 February, 2015, from http://psychcentral.com/lib/treatments-for-obsessive-compulsive-disorder/00078.

[34] Camfield, D. A., et al. (2011). "Nutraceuticals in the treatment of obsessive compulsive disorder (OCD): a review of mechanistic and clinical evidence." Prog Neuropsychopharmacol Biol Psychiatry 35(4): 887-895.

[35] Monaghan, D. T., et al. (2012). "Pharmacological modulation of NMDA receptor activity and the advent of negative and positive allosteric modulators." Neurochem Int 61(4): 581-592.

[36] Pauls, D. L. (2010). "The genetics of obsessive-compulsive disorder: a review." Dialogues Clin Neurosci 12(2): 149-163.

[37] Niciu, M. J., et al. (2014). "Glutamate receptor antagonists as fast-acting therapeutic alternatives for the treatment of depression: ketamine and other compounds." Annu Rev Pharmacol Toxicol 54: 119-139.

[38] Masi, G., et al. (2006). "Comorbidity of obsessive-compulsive disorder and attention-deficit/hyperactivity disorder in referred children and adolescents." Compr Psychiatry 47(1)

[38] Do, S. H., et al. (2002). "Effects of volatile anesthetics on glutamate transporter, excitatory amino acid transporter type 3: the role of protein kinase C." Anesthesiology 96(6): 1492-1497.

[39] Doyle, M., et al. (2014). "Obsessive compulsive symptoms in patients with Schizophrenia on Clozapine and with Obsessive Compulsive disorder: a comparison study." Compr Psychiatry 55(1): 130-136.

[40] Kobak, K. A., et al. (2005). "St. John's wort versus placebo in obsessive-compulsive disorder: results from a double-blind study." Int Clin Psychopharmacol 20(6): 299-304.

[41] Sarris, J. (2007). "Herbal medicines in the treatment of psychiatric disorders: a systematic review." Phytother Res 21(8): 703-716.

[42] Sarris, J., et al. (2011). "Herbal medicine for depression, anxiety and insomnia: a review of psychopharmacology and clinical evidence." Eur Neuropsychopharmacol 21(12): 841-860.

[43] Girdhar, S., et al. (2010). "Evaluation of anti-compulsive effect of methanolic extract of Benincasa hispida Cogn. fruit in mice." Acta Pol Pharm 67(4): 417-421.

[44] Esslinger, C. S., et al. (2005). "The substituted aspartate analogue L-beta-threo-benzyl-aspartate preferentially inhibits the neuronal excitatory amino acid transporter EAAT3." Neuropharmacology 49(6): 850-861.

[45] Vandenberg, R. J., et al. (2004). "Allosteric modulation of neurotransmitter transporters at excitatory synapses." Eur J Pharm Sci 23(1): 1-11.

[46] Abrahamsen, B., et al. (2013). "Allosteric modulation of an excitatory amino acid transporter: the subtype-selective inhibitor UCPH-101 exerts sustained inhibition of EAAT1 through an intramonomeric site in the trimerization domain." J Neurosci 33(3): 1068-1087.

[47] Alexander, S. P., et al. (2013). "The Concise Guide to PHARMACOLOGY 2013/14: transporters." Br J Pharmacol 170(8): 1706-1796.

[48] O'Neill, J., et al. (2013). "Effects of intensive cognitive-behavioral therapy on cingulate neurochemistry in obsessive-compulsive disorder." J Psychiatr Res 47(4): 494-504.

[49] Zerangue, N. and M. P. Kavanaugh (1996). "Flux coupling in a neuronal glutamate transporter." Nature 383(6601): 634-637.

[50] Jensen, A. A. and H. Brauner-Osborne (2004). "Pharmacological characterization of human excitatory amino acid transporters EAAT1, EAAT2 and EAAT3 in a fluorescence-based membrane potential assay." Biochem Pharmacol 67(11): 2115-2127.

[51] Watts, S. D., et al. (2014). "Cysteine transport through excitatory amino acid transporter 3 (EAAT3)." PLoS One 9(10): e109245.

[52] Zerangue, N. and M. P. Kavanaugh (1996). "Interaction of L-cysteine with a human excitatory amino acid transporter." J Physiol 493 (Pt 2): 419-423.

[53] Rawls, S. M. and J. F. McGinty (1998). "Kappa receptor activation attenuates L-trans-pyrrolidine-2,4-dicarboxylic acid-evoked glutamate levels in the striatum." J Neurochem 70(2): 626-634.

[54] Biasini M., Bienert S., Waterhouse A., Konstantin A., Gabriel S., Tobias S., Florian K., Tiziano Gallo Cassarino, Bertoni M., Lorenza Bordoli, Torsten Schwede. (2014). SWISS-MODEL: modelling protein tertiary and quaternary structure using evolutionary information. Nucleic Acids Research; (1 July 2014) 42 (W1): W252-W258; doi: 10.1093/nar/gku340.

[55] Jenike, M. and Dailey, S. “Sudden and Severe Onset OCD (PANS/PANDAS) – Practical Advice for Practitioners and Parents” International OCD Foundation Retrieved. 3 February 2015, from http://iocdf.org/pandas/.

[56] Shimamoto, K., et al. (2007). "Characterization of the tritium-labeled analog of L-threo-beta-benzyloxyaspartate binding to glutamate transporters." Mol Pharmacol 71(1): 294-302.

[57] Shanghai Key Laboratory. (2015) “A comprehensive source and free tool for evaluating chemical ADMET properties” ADMESTAR. Laboratory of Molecular Modeling and Desing. Retrieved from: http://lmmd.ecust.edu.cn:8000/

[58] Voth, A. R., et al. (2009). "Halogen bonds as orthogonal molecular interactions to hydrogen bonds." Nat Chem 1(1): 74-79.

[59] Scholfield, M. R., et al. (2013). "Halogen bonding (X-bonding): a biological perspective." Protein Sci 22(2): 139-152.

[60] Garrett M. Morris, David S. Goodsell, Michael E. Pique, William “Lindy” Lindstrom, Ruth Huey, Stefano Forli, William E. Hart, Scott Halliday, Rik Belew and Arthur J. Olson. AutoDock Version 4.2. Modification date: July 28, 2014 15:30 D7/P7

[61] Clark, T., et al. (2007). "Halogen bonding: the sigma-hole. Proceedings of "Modeling interactions in biomolecules II", Prague, September 5th-9th, 2005." J Mol Model 13(2): 291-296.

[62] Voth, A. R., et al. (2009). "Halogen bonds as orthogonal molecular interactions to hydrogen bonds." Nat Chem 1(1): 74-79.

[63] O'Neil, M.J. (ed.). “lidocaine” The Merck Index - An Encyclopedia of Chemicals, Drugs, and Biologicals. Cambridge, UK: Royal Society of Chemistry, 2013., p. 1019

[64] Oresman, J. V. Ortiz, Q. Cui, A. G. Baboul, S. Clifford, J. Cioslowski, B. B. Stefanov, G. Liu, A. Liashenko, P. Piskorz, I. Komaromi, R. L. Martin, D. J. Fox, T. Keith, M. A. Al-Laham, C. Y. Peng, A. Nanayakkara, M. Challacombe, P. M. W. Gill, B. Johnson, W. Chen, M. W. Wong, C. Gonzalez, and J. A. Pople, Gaussian, Inc., Wallingford CT, 2004.

[65] Lipinski, C. A. (2004). "Lead- and drug-like compounds: the rule-of-five revolution." Drug Discov Today Technol 1(4): 337-341.

[66] Petit, J., et al. (2012). "Softening the Rule of Five--where to draw the line?" Bioorg Med Chem 20(18): 5343-5351.

[67] Cavalli, A., et al. (2012). "Computational design and discovery of "minimally structured" hERG blockers." J Med Chem 55(8): 4010-4014.

[68] MacCannell D. (2014) “Window of Opportunity: In Silico Study of the Role of hERG Channel Gating in Cardiac Safety Assessment” Novartis Institutes for BioMedical Research. Retrieved from: http://www.Schrödinger.com/events/462/

[69] Zengming Zhang, Yu Li, Biaoyang Lin, Michael Schroeder and Bingding Huang (2011), Identification of cavities on protein surface using multiple computational approaches for drug binding site prediction. Bioinformatics, 27 (15): 2083-2088.

[70] Bingding Huang (2009), metaPocket: a meta approach to improve protein ligand binding site prediction , Omics, 13(4), 325-330.

[71] Chéron N, Jasty N, Shakhnovich EI. (2015) OpenGrowth: An Automated and Rational Algorithm for Finding New Protein Ligands. ACS. J Med Chem.

[72] Roy, A. Kucukural, A. Zhang Y. (2010) I-TASSER: a unified platform for automated protein structure and function prediction. Nature Protocols, 5: 725-738.

[73] Yang J, Yan R, A Roy, Xu D, Poisson J, Y Zhang. (2015)The I-TASSER Suite: Protein structure and function prediction. Nature Methods, 12: 7-8.

[74] Zhang. Y. (2008) I-TASSER server for protein 3D structure prediction. BMC Bioinformatics, vol 9, 40.

[75] Yang y., Yaoqi Zhou. (2008) Specific interactions for ab initio folding of protein terminal regions with secondary structures. Proteins,72(2):793-803.

[75] Mas, S., et al. (2014). "Role of GAD2 and HTR1B genes in early-onset obsessive-compulsive disorder: results from transmission disequilibrium study." Genes Brain Behav 13(4): 409-417.

[76] Biasini M., Bienert S., Waterhouse A., Konstantin A., Gabriel S., Tobias S., Florian K., Tiziano Gallo Cassarino, Bertoni M., Lorenza Bordoli, Torsten Schwede. (2014). SWISS-MODEL: modelling protein tertiary and quaternary structure using evolutionary information. Nucleic Acids Research; (1 July 2014) 42 (W1): W252-W258; doi: 10.1093/nar/gku340.

[77] Guex, N., Peitsch, M.C., Schwede, T. (2009). Automated comparative protein structure modeling with SWISS-MODEL and Swiss-PdbViewer: A historical perspective. Electrophoresis, 30(S1), S162-S173.

[78] Kiefer F, Arnold K, Künzli M, Bordoli L, Schwede T (2009). The SWISS-MODEL Repository and associated resources. Nucleic Acids Research. 37, D387-D392.

[79] U.S. National Library of Medicine "LIDOCAINE" CASRN: 137586. Retrieved 1 April, 2015 from http://www.ncbi.nlm.nih.gov/pubmedhealth/PMHT0001058.

[80] ACD/Structure Elucidator, (2014) version 12.01, “Advanced Chemistry Development, Inc.”, Toronto, ON, Canada, retrieved from: www.acdlabs.com.

[81] American Society of Health-System Pharmacists 2014; Drug Information. "lidocaine" 2014. Bethesda, MD. 2014, p. 1697

[82] Benkert P, Künzli M, Schwede T. (2009). "QMEAN Server for Protein Model Quality Estimation." Nucleic Acids Res. 2009 Jul 1;37(Web Server issue):W510-4

[83] Bhattacharya D. and Cheng J. 3Drefine: Consistent Protein Structure Refinement by Optimizing Hydrogen- Bonding Network and Atomic-Level Energy Minimization. Proteins: Structure, Function and Bioinformatics. 2012

[84] Kelley, L. A., et al. (2015). "The Phyre2 web portal for protein modeling, prediction and analysis." Nat. Protocols 10(6): 845-858.

[85] Yang Y., Yaoqi Zhou. Ab initio folding of terminal segments with secondary structures reveals the fine difference between two closely related all-atom statistical energy functions.Protein Science,17:1212-1219(2008)

[86] Narayanan E., Pieper U., Webb B. et al (2015). ModWeb: A Server for Protein Structure Modeling. from: https://modbase.compbio.ucsf.edu/modweb/

[87] Schwede, T., Kopp, J., Guex, N. and Peitsch, M.C. (2003) SWISS-MODEL: an automated protein homology-modeling server. Nucleic Acids Res., 31,3381-3385.

APPENDIX

A.1. EAAT3 Amino Acid Sequence.

The sequence used for the calculations was taken from the protein data bank, which corresponds to the EAA3_HUMAN Excitatory amino acid transporter 3, derived from the gene SLC1A1. The sequence is the following:

MGKPARKGCEWKRFLKNNWVLLSTVAAVVLGITTGVLVREHSNLSTLEKFYFAFPGEILM

RMLKLIILPLIISSMITGVAALDSNVSGKIGLRAVVYYFCTTLIAVILGIVLVVSIKPGV

TQKVGEIARTGSTPEVSTVDAMLDLIRNMFPENLVQACFQQYKTKREEVKPPSDPEMNMT

EESFTAVMTTAISKNKTKEYKIVGMYSDGINVLGLIVFCLVFGLVIGKMGEKGQILVDFF

NALSDATMKIVQIIMCYMPLGILFLIAGKIIEVEDWEIFRKLGLYMATVLTGLAIHSIVI

LPLIYFIVVRKNPFRFAMGMAQALLTALMISSSSATLPVTFRCAEENNQVDKRITRFVLP

VGATINMDGTALYEAVAAVFIAQLNDLDLGIGQIITISITATSASIGAAGVPQAGLVTMV

IVLSAVGLPAEDVTLIIAVDWLLDRFRTMVNVLGDAFGTGIVEKLSKKELEQMDVSSEVN

IVNPFALESTILDNEDSDTKKSYVNGGFAVDKSDTISFTQTSQF

A.2. Homology Structure Modeling of EAAT3

In the I-TASSER, the LOMET (Local Meta-Threading) server retrieves a template of proteins with similar folds. Thereafter, the program retrieves fragments excised from the PDB templates and reassembles them into full-length models by replica-exchange Monte Carlo simulations. The unaligned regions are resolved by ab-initio models. Once the structure has been assembled, low free-energy states are identified by SPICKER (clustering algorithm to identify the

near-native models from protein structure decoys). The final step in this process is to remove the steric clash, as well as to refine the global topology of the cluster centroids using TM align.[73,74,75]

In Modweb we produced 2 different models based on different algorithms. The first protein model was derived from the provided amino acid sequence. Using PSI-BLAST (Position-Specific Iterated BLAST) the sequence was scanned against all profiles in the template profile database to find hits; it then used position-specific scoring matrices (PSSMs) to score matches between query and database sequences to make the model construct. The second model was built with the HHBlits algorithm, which is based on the pairwise alignment of hidden Markov models (HMMs). First it searches for a multiple sequence alignment in databases for homologous proteins; then the HHblits can build high-quality multiple sequence alignment starting from single sequences.[86]

In the Schodinger Maestro, the sequence homology is based on the provided sequence alignment and a provided PBD structure. We selected 2 PDB structures (PDB ID: 4P19 and 2NWX) and to make our models, the algorithm used was the Prime STA method, which is best suited for low sequence identity.

Phyre 2 uses the alignment of HMMs via HHsearch1 to significantly improve accuracy of alignment and detection rate. Phyre2 also incorporates an ab-initio folding simulation called Poing2 to model regions of the proteins with no detectable homology. [84]

In the swiss model server, the server automatically searches for structures based on Blast and HHblits. Once the sequence alignment and the first structure is modeled, the server optimizes the top-ranking templates using PROMOD-II and MODELLER.[87]

Table 12. Model quality estimation for the EAAT3 protein.

Protein Model Name	QMEAN-Score	OPT. models QMEAN-Score	Z-Score (dDfire/dDFIRE2)	OPT. models Z-Score (dDfire/DFIRE2)
I-Tasser Model 1	0.414	0.414	-4.15 (-1190.09/ -949.704)	-3.88 (-1189.71/ -949.674)
I-Tasser Model 2	0.399	0.400	-4.32 (-1169.96 /-942.074)	-4.04 (-1169.67 /-941.909)
I-Tasser Model 3	0.418	0.418	-4.1 (-1169.67 /-941.909)	-3.84 (-1161.26 /-948.421)
I-Tasser Model 4	0.407	0.407	-4.23 (-1184.37 /-966.396)	-3.96 (-1184.13 /-966.399)
I-Tasser Model 5	0.483	0.483	-3.33 (-1224.74 /-963.67)	-3.33 (-1224.86 /-963.615)
Modbase PSI Model 1	0.377	0.348	-4.65 (-1058.44 /-823.483)	-4.75 (-1059.05 /-823.756)
Modbase PSI Model 2	0.443	0.436	-3.66 (-1040.50 /-788.957)	-3.74 (-1039.74 /-788.987)
Modbase PSI Model 3	0.441	0.437	-3.70 (-1043.23 /-821.786)	-3.74 (-1043.88 /-821.787)
Modbase HHBlits Model 1	0.358	0.355	-4.88 (-1049.64 /-824.254)	-4.67 (-1049.84 /-824.13)
Schrödinger Model 1	0.433	0.466	-3.81 (-1021.19 /-770.618)	-3.42 (-1021.09 /-770.487)
Schrödinger 2NWX Model	0.527	0.531	-2.51 (-3054.53 /-2906.31)	-2.47 (-3085.75 /-2438.23)
Schrödinger 4P19 Model	Structure could not be process	0.635	Structure could not be process	-1.332 (-3373.50 /-2601.08)
Phyre2 C4KY Model	0.411	0.455	-4.19 (-1021.14 /-770.642)	-3.55 (-1021.04 /-770.512)

Phyre2 Model	0.415	0.466	-4.15 (-1021.19 /-770.618)	-3.42 (-1021.09 /-770.487)
Phyre2 Intensive Model	0.395	0.383	-4.37 (-1233.86 / -952.311)	-4.23 (-1234.65 / -952.43)
Swiss Model 1	0.519	0.530	-2.74 (-3207.98 /-2588.56)	-2.62 (-3206.86 /-2588.89)
Swiss Model 2	0.500	0.513	-2.99 (-3228.08 /-2554.32)	-2.83 (-2.83 -3226.09 /-2554.31)
Swiss Model 3	0.479	0.491	-3.16 (-3281.35 /-2594.54)	-3.02 (-3282.90 /-2594.56)

Table 13. Protein models and Ramachandran plots.

Protein Model Name	Model	Ramachandran Plot
I-Tasser Model 1	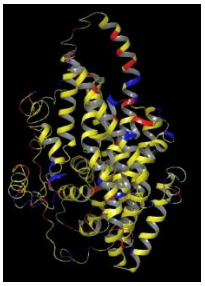	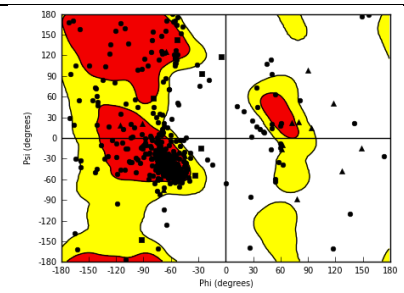
I-Tasser Model 2		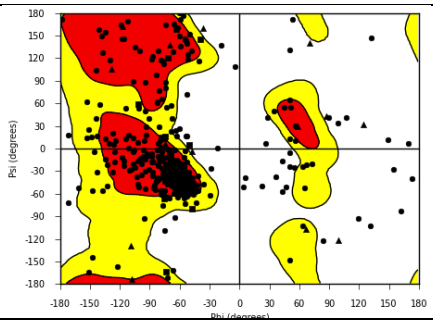

I-Tasser Model 3		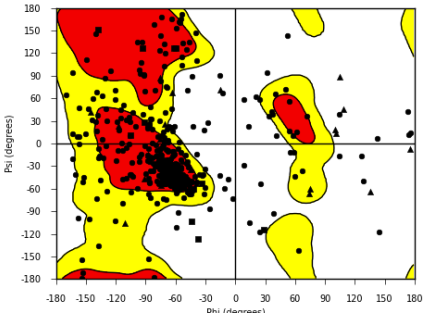
I-Tasser Model 4	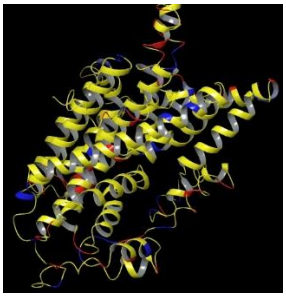	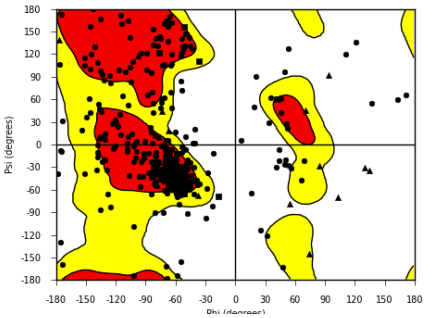
I-Tasser Model 5	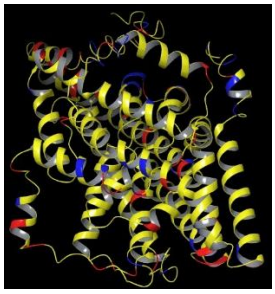	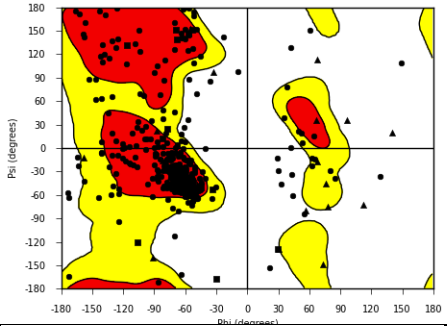
Modbase PSI Model 1	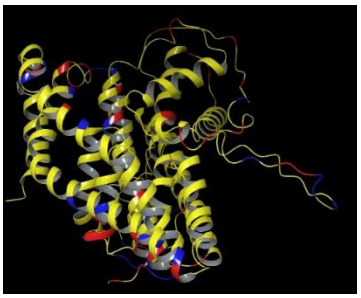	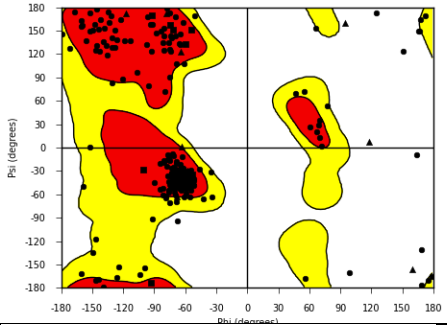
Modbase PSI Model 2	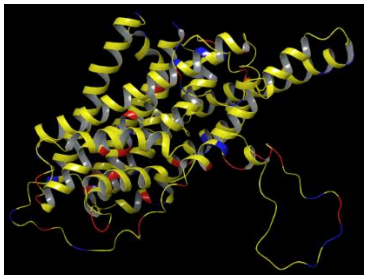	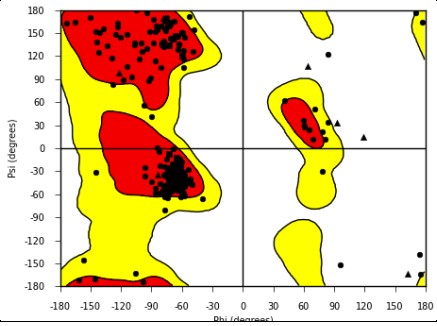

Modbase PSI Model 3	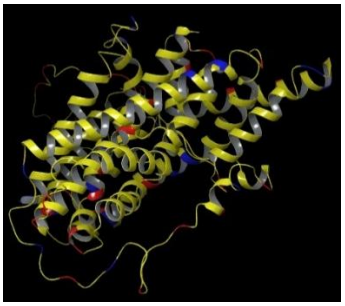	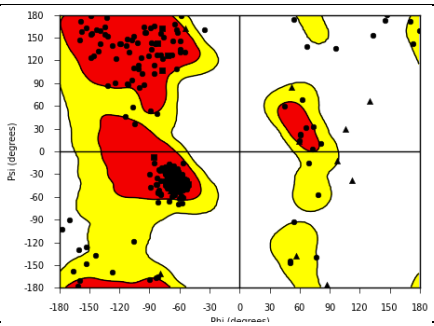
Modbase HHBlits Model 1	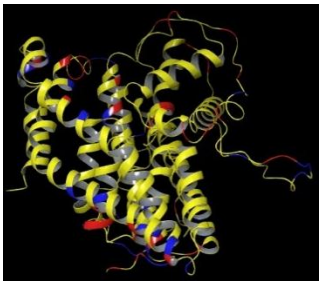	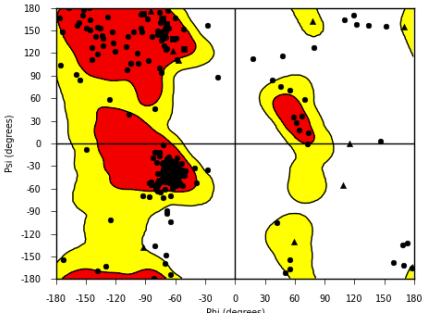
Schrödinger Model 1	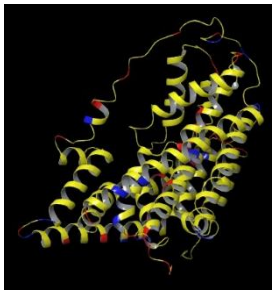	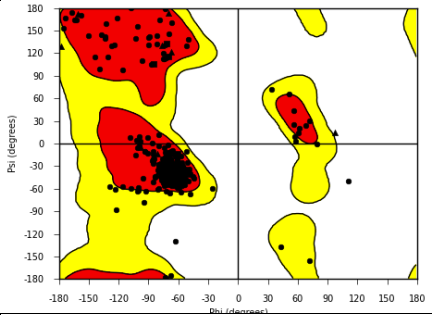
Schrödinger 2NWX Model	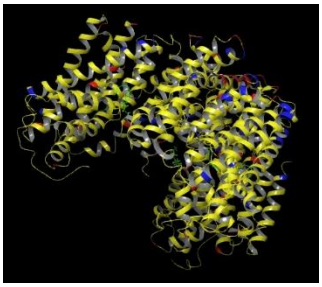	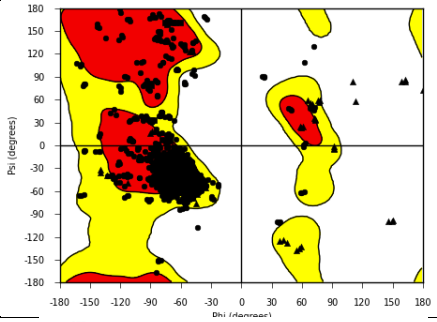
Schrödinger 4P19 Model	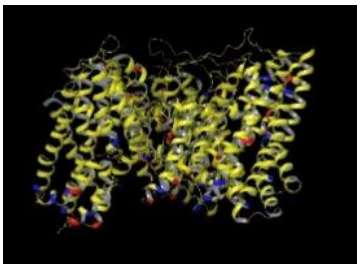	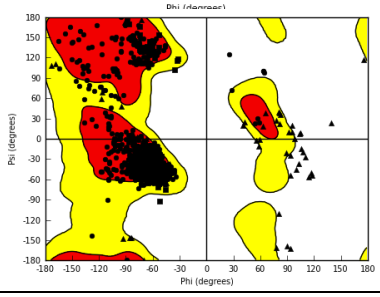

Phyre2 C4KY Model	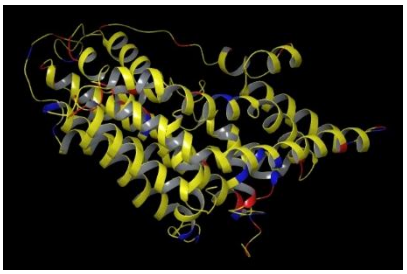	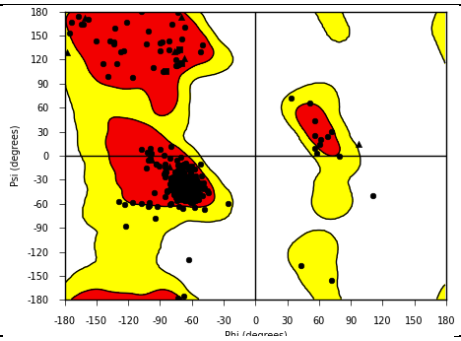
Phyre2 Model	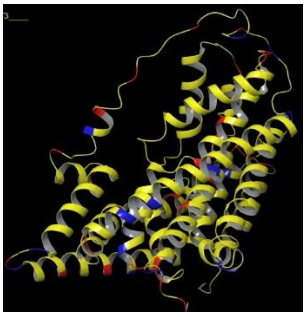	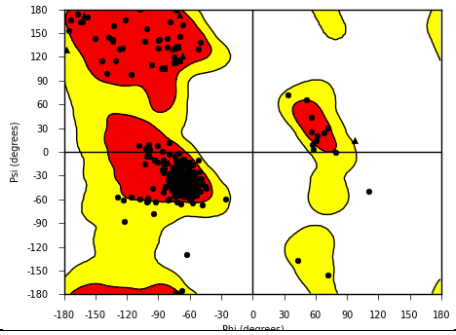
Phyre2 Intensive Model	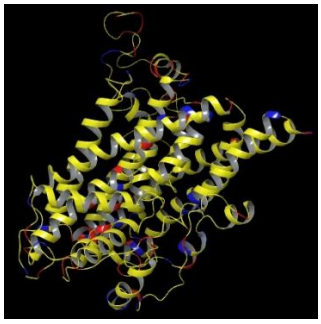	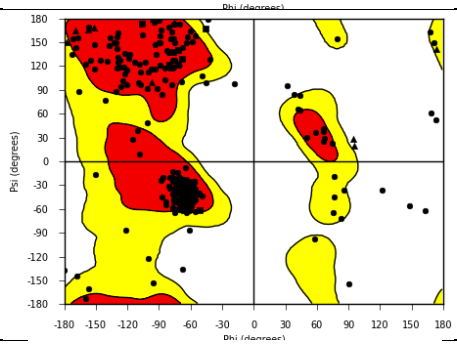
Swiss Model 1	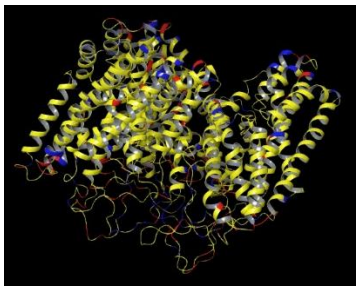	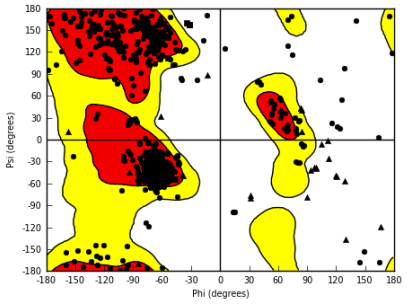
Swiss Model 2	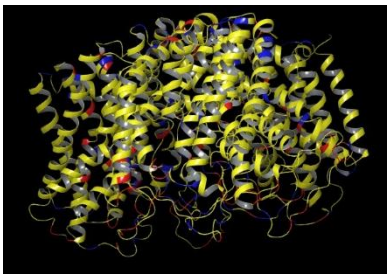	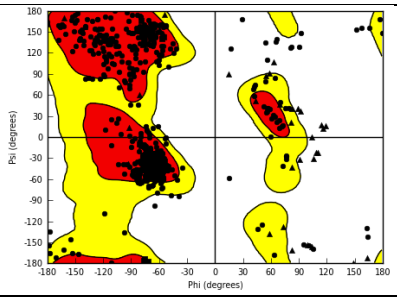

Swiss Model 3	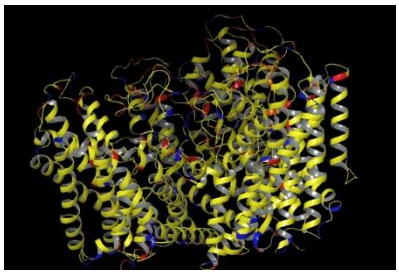	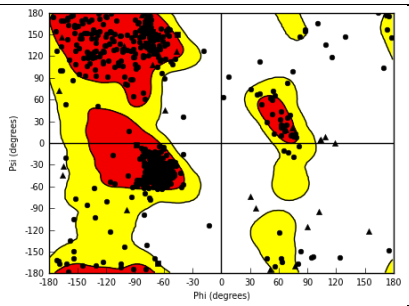

A.3. Molecular Structures and Calculated Physico-Chemical Properties

Lipinski-type properties and ADMET of Lidocaine:

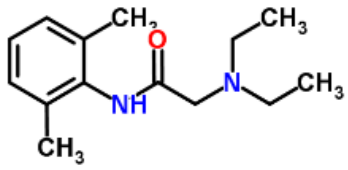

- Molecular Weight: 234.34
- No. of Hydrogen Bond Donors: 1
- No. of Hydrogen Bond Acceptors: 3
- Total Polar Surface Area: 32.34
- No. of Rotatable Bonds: 5

Model	Result	Probability
Absorption		
Blood-Brain Barrier	BBB+	0.8917
Human Intestinal Absorption	HIA+	0.9737
Caco-2 Permeability	Caco2+	0.8867
P-glycoprotein Substrate	Substrate	0.6680
P-glycoprotein Inhibitor	Non-inhibitor	0.8781
	Non-inhibitor	0.9824
Renal Organic Cation Transporter	Non-inhibitor	0.8308
Metabolism		
CYP450 2C9 Substrate	Non-substrate	0.7721
CYP450 2D6 Substrate	Substrate	0.8919
CYP450 3A4 Substrate	Substrate	0.5735
CYP450 1A2 Inhibitor	Non-inhibitor	0.9046
CYP450 2C9 Inhibitor	Non-inhibitor	0.9231
CYP450 2D6 Inhibitor	Non-inhibitor	0.9231
CYP450 2C19 Inhibitor	Non-inhibitor	0.9026
CYP450 3A4 Inhibitor	Non-inhibitor	0.9394
CYP Inhibitory Promiscuity	High CYP Inhibitory Promiscuity	0.5770

Toxicity		
Human Ether-a-go-go-Related Gene Inhibition	Weak inhibitor	0.9501
	Non-inhibitor	0.8604
AMES Toxicity	Non AMES toxic	0.8315
Carcinogens	Carcinogens	0.5208
Fish Toxicity	High FHMT	0.5284
Tetrahymena Pyriformis Toxicity	High TPT	0.8455
Honey Bee Toxicity	Low HBT	0.8925
Biodegradation	Not ready biodegradable	0.9948
Acute Oral Toxicity	II	0.7397
Carcinogenicity (Three-class)	Non-required	0.7165
Other Predicted Toxicity Values		
Model	Value	Unit
Aqueous solubility (Absorption)	-1.8221	LogS
Caco-2 Permeability (Absorption)	1.7551	LogPapp, cm/s
Rat Acute Toxicity	2.8382	LD50, mol/kg
Fish Toxicity	1.5030	pLC50, mg/L
Tetrahymena Pyriformis Toxicity	0.4246	pIGC50, ug/L

Lipinski-type properties and ADME of LA 1:

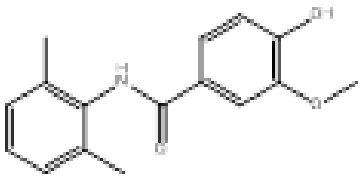

- Molecular Weight: 271.31
- No. of Hydrogen Bond Donors: 2
- No. of Hydrogen Bond Acceptors: 4
- No. of Rotatable Bonds: 3
- QPlogHERG: 12

Model	Result	Probability
Absorption		
Blood-Brain Barrier	BBB+	0.8023
Human Intestinal Absorption	HIA+	0.9716
Caco-2 Permeability	Caco2+	0.7682
Metabolism		
CYP450 2C9 Substrate	Non-substrate	0.7268
CYP450 2D6 Substrate	Non-substrate	0.5174
CYP450 3A4 Substrate	Substrate	0.6194
CYP450 1A2 Inhibitor	Non-inhibitor	0.6825
CYP450 2C9 Inhibitor	Non-inhibitor	0.9084
CYP450 2D6 Inhibitor	Non-inhibitor	0.9206

CYP450 2C19 Inhibitor	Non-inhibitor	0.8486
CYP450 3A4 Inhibitor	Non-inhibitor	0.6184
CYP Inhibitory Promiscuity	High CYP Inhibitory Promiscuity	0.5000
Toxicity		
Human Ether-a-go-go-Related Gene Inhibition	Weak inhibitor	0.9935
	Non-inhibitor	0.7257
AMES Toxicity	Non AMES toxic	0.5000
Carcinogens	Non-carcinogens	0.8006
Fish Toxicity	High FHMT	0.6417
Tetrahymena Pyriformis Toxicity	High TPT	0.9385
Honey Bee Toxicity	Low HBT	0.6572
Biodegradation	Not ready biodegradable	0.9617
Acute Oral Toxicity	III	0.5351
Carcinogenicity (Three-class)	Non-required	0.4405
Other Predicted Toxicity Values		
Model	Value	Unit
Aqueous solubility (Absorption)	-3.2583	LogS
Caco-2 Permeability (Absorption)	1.4032	LogPapp, cm/s
Rat Acute Toxicity	2.0836	LD50, mol/kg
Fish Toxicity	1.3803	pLC50, mg/L
Tetrahymena Pyriformis Toxicity	1.0061	pIGC50, ug/L

Lipinski-type properties and ADME of LA 2:

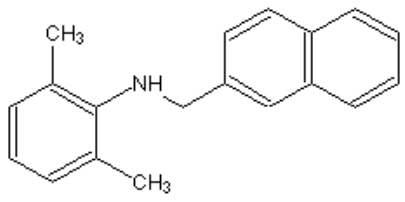

- Molecular Weight: 261.36
- No. of Hydrogen Bond Donors: 1
- No. of Hydrogen Bond Acceptors: 1
- No. of Rotatable Bonds: 3
- QPlogHERG: 16

Model	Result	Probability
Absorption		
Blood-Brain Barrier	BBB+	0.9842
Human Intestinal Absorption	HIA+	0.9946
Caco-2 Permeability	Caco2+	0.7507

Metabolism		
CYP450 2C9 Substrate	Non-substrate	0.7758
CYP450 2D6 Substrate	Non-substrate	0.5302
CYP450 3A4 Substrate	Substrate	0.5635
CYP450 1A2 Inhibitor	Non-inhibitor	0.9076
CYP450 2C9 Inhibitor	Inhibitor	0.5509
CYP450 2D6 Inhibitor	Inhibitor	0.6086
CYP450 2C19 Inhibitor	Inhibitor	0.8733
CYP450 3A4 Inhibitor	Non-inhibitor	0.6568
CYP Inhibitory Promiscuity	High CYP Inhibitory Promiscuity	0.8717
Toxicity		
Human Ether-a-go-go-Related Gene Inhibition	Weak inhibitor	0.8793
	Non-inhibitor	0.6208
AMES Toxicity	AMES toxic	0.7396
Carcinogens	Non-carcinogens	0.5977
Fish Toxicity	High FHMT	0.9051
Tetrahymena Pyriformis Toxicity	High TPT	0.9971
Honey Bee Toxicity	Low HBT	0.6551
Biodegradation	Not ready biodegradable	0.9630
Acute Oral Toxicity	III	0.6737
Carcinogenicity (Three-class)	Non-required	0.6200
Other Predicted Toxicity Values		
Model	Value	Unit
Aqueous solubility (Absorption)	-4.3896	LogS
Caco-2 Permeability (Absorption)	1.6271	LogPapp, cm/s
Rat Acute Toxicity	2.6708	LD50, mol/kg
Fish Toxicity	0.8761	pLC50, mg/L
Tetrahymena Pyriformis Toxicity	0.7795	pIGC50, ug/L

Lipinski-type properties and ADME of LA 3:

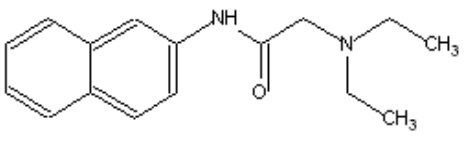

- Molecular Weight: 256.34
- No. of Hydrogen Bond Donors: 1
- No. of Hydrogen Bond Acceptors: 3
- No. of Rotatable Bonds: 5
- QPlogHERG: 10

Model	Result	Probability
Absorption		
Blood-Brain Barrier	BBB+	0.9821
Human Intestinal Absorption	HIA+	1.0000
Caco-2 Permeability	Caco2+	0.6313
Metabolism		
CYP450 2C9 Substrate	Non-substrate	0.7536
CYP450 2D6 Substrate	Non-substrate	0.5508
CYP450 3A4 Substrate	Non-substrate	0.5562
CYP450 1A2 Inhibitor	Inhibitor	0.6757
CYP450 2C9 Inhibitor	Non-inhibitor	0.6532
CYP450 2D6 Inhibitor	Non-inhibitor	0.7723
CYP450 2C19 Inhibitor	Non-inhibitor	0.5687
CYP450 3A4 Inhibitor	Non-inhibitor	0.8327
CYP Inhibitory Promiscuity	High CYP Inhibitory Promiscuity	0.8074
Toxicity		
Human Ether-a-go-go-Related Gene Inhibition	Weak inhibitor	0.7965
	Non-inhibitor	0.6751
AMES Toxicity	Non AMES toxic	0.5859
Carcinogens	Non-carcinogens	0.6267
Fish Toxicity	High FHMT	0.8763
Tetrahymena Pyriformis Toxicity	High TPT	0.9964
Honey Bee Toxicity	Low HBT	0.7797
Biodegradation	Not ready biodegradable	0.9880
Acute Oral Toxicity	III	0.6021
Carcinogenicity (Three-class)	Non-required	0.6077
Other Predicted Toxicity Values		
Model	Value	Unit
Aqueous solubility (Absorption)	-4.3985	LogS
Caco-2 Permeability (Absorption)	1.7201	LogPapp, cm/s
Rat Acute Toxicity	2.2839	LD50, mol/kg
Fish Toxicity	1.5225	pLC50, mg/L
Tetrahymena Pyriformis Toxicity	0.9096	pIGC50, ug/L

Lipinski-type properties and ADME of LA 4:

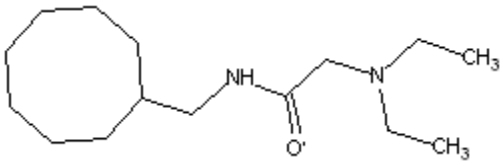

- Molecular Weight: 254.41
- No. of Hydrogen Bond Donors: 1
- No. of Hydrogen Bond Acceptors: 3
- No. of Rotatable Bonds: 6
- QPlogHERG: 8

Model	Result	Probability
Absorption		
Blood-Brain Barrier	BBB+	0.9783
Human Intestinal Absorption	HIA+	0.9957
Caco-2 Permeability	Caco2+	0.6397
Metabolism		
CYP450 2C9 Substrate	Non-substrate	0.8599
CYP450 2D6 Substrate	Non-substrate	0.573
CYP450 3A4 Substrate	Non-substrate	0.5886
CYP450 1A2 Inhibitor	Non-inhibitor	0.8246
CYP450 2C9 Inhibitor	Non-inhibitor	0.9288
CYP450 2D6 Inhibitor	Non-inhibitor	0.8135
CYP450 2C19 Inhibitor	Non-inhibitor	0.8535
CYP450 3A4 Inhibitor	Non-inhibitor	0.9113
CYP Inhibitory Promiscuity	Low CYP Inhibitory Promiscuity	0.817
Toxicity		
Human Ether-a-go-go-Related Gene Inhibition	Weak inhibitor	0.9019
	Non-inhibitor	0.8388
AMES Toxicity	Non AMES toxic	0.8182
Carcinogens	Non-carcinogens	0.6846
Fish Toxicity	Low FHMT	0.6612
Tetrahymena Pyriformis Toxicity	High TPT	0.725
Honey Bee Toxicity	Low HBT	0.7618
Biodegradation	Not ready biodegradable	0.9873
Acute Oral Toxicity	III	0.7417
Carcinogenicity (Three-class)	Non-required	0.7178
Other Predicted Toxicity Values		
Model	**Value**	**Unit**
Aqueous solubility (Absorption)	-1.888	LogS
Caco-2 Permeability (Absorption)	1.2964	LogPapp, cm/s
Rat Acute Toxicity	2.171	LD50, mol/kg
Fish Toxicity	2.1055	pLC50, mg/L
Tetrahymena Pyriformis Toxicity	-0.1532	pIGC50, ug/L

Lipinski-type properties and ADME of LA 5:

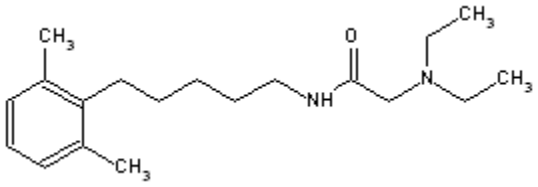

- Molecular Weight: 304.47
- No. of Hydrogen Bond Donors: 1
- No. of Hydrogen Bond Acceptors: 3
- No. of Rotatable Bonds: 10
- QPlogHERG: 6

Model	Result	Probability
Absorption		
Blood-Brain Barrier	BBB+	0.8904
Human Intestinal Absorption	HIA+	0.9917
Caco-2 Permeability	Caco2+	0.7302
Metabolism		
CYP450 2C9 Substrate	Non-substrate	0.8126
CYP450 2D6 Substrate	Substrate	0.6501
CYP450 3A4 Substrate	Non-substrate	0.5056
CYP450 1A2 Inhibitor	Non-inhibitor	0.8419
CYP450 2C9 Inhibitor	Non-inhibitor	0.9501
CYP450 2D6 Inhibitor	Non-inhibitor	0.5875
CYP450 2C19 Inhibitor	Non-inhibitor	0.8566
CYP450 3A4 Inhibitor	Non-inhibitor	0.8007
CYP Inhibitory Promiscuity	Low CYP Inhibitory Promiscuity	0.761
Toxicity		
Human Ether-a-go-go-Related Gene Inhibition	Weak inhibitor	0.871
	Inhibitor	0.5
AMES Toxicity	Non AMES toxic	0.9006
Carcinogens	Non-carcinogens	0.6906
Fish Toxicity	High FHMT	0.5798
Tetrahymena Pyriformis Toxicity	High TPT	0.985
Honey Bee Toxicity	Low HBT	0.8517
Biodegradation	Not ready biodegradable	0.9846
Acute Oral Toxicity	III	0.7636
Carcinogenicity (Three-class)	Non-required	0.7498
Other Predicted Toxicity Values		
Model	**Value**	**Unit**
Aqueous solubility (Absorption)	-2.3317	LogS

Caco-2 Permeability(Absorption)	1.4992	LogPapp, cm/s
Rat Acute Toxicity	2.1784	LD50, mol/kg
Fish Toxicity	1.588	pLC50, mg/L
Tetrahymena Pyriformis Toxicity	0.2639	pIGC50, ug/L

Lipinski-type properties and ADME of LA 6:

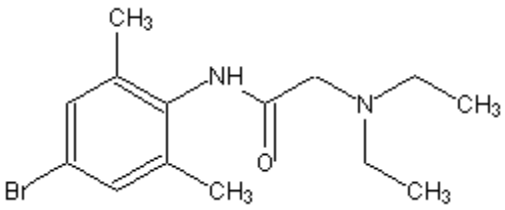

- Molecular Weight: 313.23
- No. of Hydrogen Bond Donors: 1
- No. of Hydrogen Bond Acceptors: 3
- No. of Rotatable Bonds: 5
- QPlogHERG: 6

Model	Result	Probability
Adsorption		
Blood-Brain Barrier	BBB+	0.9142
Human Intestinal Absorption	HIA+	0.9672
Caco-2 Permeability	Caco2+	0.7793
Metabolism		
CYP450 2C9 Substrate	Non-substrate	0.8139
CYP450 2D6 Substrate	Non-substrate	0.7012
CYP450 3A4 Substrate	Substrate	0.6031
CYP450 1A2 Inhibitor	Non-inhibitor	0.6173
CYP450 2C9 Inhibitor	Non-inhibitor	0.7425
CYP450 2D6 Inhibitor	Non-inhibitor	0.8724
CYP450 2C19 Inhibitor	Non-inhibitor	0.7808
CYP450 3A4 Inhibitor	Inhibitor	0.915
CYP Inhibitory Promiscuity	High CYP Inhibitory Promiscuity	0.8153
Toxicity		
Human Ether-a-go-go-Related Gene Inhibition	Weak inhibitor	0.9551
	Inhibitor	0.73
AMES Toxicity	Non AMES toxic	0.8292
Carcinogens	Non-carcinogens	0.5104
Fish Toxicity	High FHMT	0.7691
Tetrahymena Pyriformis Toxicity	High TPT	0.9901
Honey Bee Toxicity	Low HBT	0.9101
Biodegradation	Not ready biodegradable	1

Acute Oral Toxicity	III	0.5332
Carcinogenicity (Three-class)	Non-required	0.6517
Other Predicted Toxicity Values		
Model	**Value**	**Unit**
Aqueous solubility (Absorption)	-2.8825	LogS
Caco-2 Permeability (Absorption)	1.6828	LogPapp, cm/s
Rat Acute Toxicity	2.6554	LD50, mol/kg
Fish Toxicity	1.2685	pLC50, mg/L
Tetrahymena Pyriformis Toxicity	1.0022	pIGC50, ug/L

CURRICULUM VITA

Emmanuel Zubia Salgado was born in Cd. Juarez, Chihuahua, Mexico. He is a creative and curious individual who is always interested in learning about the biochemical processes occurring in nature. The pursue of this knowledge led him to obtain a bachelor's degree in chemistry from the University of Texas at El Paso. During the last semester of his bachelor's degree, he engaged in research at a biochemical laboratory performing a protein binding experiment, which motivated him to pursue a graduate degree. In 2010 he got into the Chemistry Master's program at the same university. In late 2012 he decided to continue and expand his research, so he switched to the Chemistry PhD. program. During the tenure of his PhD he received second place for the Best Chemistry Platform Presentation during Chemistry Day, and due to his excellent skills as a teaching assistant, he was temporarily placed as the Coordinator Supervisor for the General Chemistry laboratories while the Chemistry Department hired a replacement. In the last semester of his PhD., he was forced to resign from the PhD because two professors in his committee did not agree with his proposal B idea. On the fall of 2015, Emmanuel decided to move forward and complete his master's degree with a developed idea from his PhD proposal B. To date he is very grateful to his wife, family, friends, research mentor, the Chemistry Assistant Chair and Chemistry Chair for their support and help during this ordeal. Emmanuel Zubia Salgado plans to continue his studies in the field of Environmental Science and Engineering.

Permanent address: Retorno del Granero #6917

Cd. Juarez, Chihuahua, Mexico, 32507

This thesis/dissertation was typed by: Emmanuel Zubia Salgado